The Cpx stress response regulates turnover of respiratory chain proteins at the inner

membrane of *Escherichia coli.*

by

Valeria Tsviklist

A thesis submitted in partial fulfillment of the requirements for the degree of

Master of Science

in

MICROBIOLOGY AND BIOTECHNOLOGY

DEPARTMENT OF BIOLOGICAL SCIENCES

University of Alberta

ABSTRACT

The cell envelope of Gram-negative bacteria is a unique multilayered structure that protects them from the constantly changing and often times inhospitable environments, and significantly contributes to their virulence. Having a complex structure, it requires an extensive regulatory network to monitor its assembly and stability. *Escherichia coli* possess an array of two-component signal transduction systems, some of which respond to cell envelope perturbations, including loss of proton-motive force, peptidoglycan stress, outer and inner membrane biogenesis defects. The Cpx envelope stress response is one of the major signaling pathways monitoring bacterial envelope integrity, activated both internally by excessive synthesis of membrane proteins and externally by a variety of environmental cues. The Cpx regulon is enriched with genes coding for protein folding and degrading factors, virulence determinants, large envelope-localized complexes and small regulatory RNAs. The Cpx response has been linked to a number of essential cellular processes, including iron sequestration, solute transport and cellular respiration. Transcriptional repression of the two electron transport chain complexes, NADH dehydrogenase I and cytochrome *bo3*, by the Cpx pathway has been demonstrated, however, there is evidence that additional regulatory mechanisms exist. The purpose of this thesis was to examine the interaction between Cpx-regulated protein folding and degrading factors and the respiratory complexes NADH dehydrogenase I and succinate dehydrogenase in *Escherichia coli*. Previously performed microarray analysis demonstrated that genes coding for succinate dehydrogenase complex were downregulated in the presence of the induced Cpx response. Here, we validate the microarray results and show that the succinate dehydrogenase complex has reduced activity in *E. coli* lacking the Cpx pathway and is most likely transcriptionally downregulated by the Cpx response. Furthermore, we demonstrate that the stability of the NADH dehydrogenase I protein complex is lower in cells with a functional Cpx response, while in its absence, protein turnover

is impaired. We provide evidence that Cpx-regulated envelope quality control factors are involved in the biogenesis and turnover of the respiratory complexes. Next, we demonstrate that the cellular need for Cpx-mediated stress adaptation increases when respiratory complexes are more prevalent or active, which is demonstrated by the growth defect of Cpx-deficient strains on media that requires a functional electron transport chain. Interestingly, deletion of several Cpx-regulated proteolytic factors and chaperones resulted in similar growth-deficient phenotypes. Finally, we have found that increased expression of the small regulatory RNA CpxQ, whose production is strongly upregulated upon Cpx induction, leads to stabilization or increased transcription of the *sdhC* transcript. Together, our results demonstrate that the Cpx two-component system has a broader function in surveillance of the cell envelope, regulating the abundance of large envelope protein complexes. It mounts a complex and balanced response to envelope damage, allowing effective recovery from the envelope stress and maintaining the cellular energy status of the cell.

PREFACE

Content presented in this thesis has been accepted for publication as Valeria Tsviklist, Randi L. Guest and Tracy L. Raivio "The Cpx stress response regulates turnover of respiratory chain proteins at the inner membrane of *Escherichia coli*", 2021, Front. Microbiol. - Microbial Physiology and Metabolism.

I was responsible for collection and analysis of all the data present in this thesis. I also was responsible for all the writing in this thesis. TL Raivio was involved with the design of the study, thesis composition, and edits.

ACKNOWLEDGMENTS

TABLE OF CONTENTS

LIST OF TABLES

LIST OF FIGURES

LIST OF SYMBOLS, NOMENCLATURE, AND ABBREVIATIONS

Symbols

Δ: Deletion of the specified gene locus

:: Interruption of the genetic locus by insertion

Abbreviations

A_{600}: absorbance at 600nm

Amk: amikacin

Amp: ampicillin

ATP: adenosine triphosphate

Cam: chloramphenicol

CP: cytoplasm

DNA: deoxyribonucleic acid

FAD: Flavin adenine dinucleotide

$FADH_2$: Flavin adenine dinucleotide (reduced form)

Fe: iron

FMN: Flavin mononucleotide

GDP: guanosine diphosphate

GTP: guanosine triphosphate

IM: inner membrane

IPTG: isopropyl-β-D-thiogalactopyranoside

Kan: kanamycin

LPS: lipopolysaccharide

mRNA: messenger RNA

NAD: Nicotinamide adenine dinucleotide

NADH: Nicotinamide adenine dinucleotide (reduced form)

NDH: NADH dehydrogenase

OD_{600}: optical density at 600nm

OM: outer membrane

PG: peptidoglycan

PMF: proton motive force

Q: quinone

QH_2: quinol

SDH: succinate dehydrogenase

RBS: ribosomal binding site

RNA: ribonucleic acid

S: sulfur

SDH: succinate dehydrogenase

SDS-PAGE: sodium dodecyl sulfate polyacrylamide gel electrophoresis

sRNA: small RNA

TIR: translation initiation region

WT: wildtype

INTRODUCTION

Escherichia coli

Commensal *Escherichia coli* (*E. coli*) is one of the best studied bacterial organisms used as a model in molecular biology and biotechnology research. Due to plasticity of its genome, *E. coli* can be utilized in cloning and expression of foreign genes thus has demonstrable versatility as a tool for genetic engineering (1). These gram-negative bacteria live as commensals in the gastrointestinal tract of warm-blooded animals and reptiles, colonizing the large intestine and residing within the mucus layer (2). *E. coli* are facultative anaerobes and therefore possess an ability to grow both aerobically using oxygen as a terminal electron acceptor, anaerobically using an alternative terminal electron acceptor, or by fermentation (3). Facultative anaerobic gut commensals such as *E. coli*, which constitute about 0.1% of the gut microbiota, promote normal intestinal homeostasis and help prevent colonization by pathogens (4). However some *E. coli* strains have acquired a combination of virulence factors that enable them to cause infections that may be limited to the mucosal surfaces or can disseminate throughout the body (5). Three general clinical syndromes result from infection with pathogenic *E. coli* strains: (i) urinary tract infections, (ii) sepsis/meningitis, and (iii) enteric/diarrheal disease (5). Six known pathotypes of *E. coli* including enteropathogenic *E. coli* (EPEC), enterohaemorrhagic *E. coli* (EHEC), enterotoxigenic *E. coli* (ETEC), enteroaggregative *E. coli* (EAEC), enteroinvasive *E. coli* (EIEC), and adherent-invasive *E. coli* (AIEC) are known to cause the aforementioned diseases.

The Gram-Negative Bacterial Envelope

During their lifecycle, pathogenic bacteria encounter numerous harsh and frequently changing environments, including pH, temperature, and oxygen level fluctuations, as well as a variety of host defense mechanisms such as antimicrobial compounds and the cells of the immune system. To be able to withstand these conditions and successfully colonize their hosts,

Gram-negative bacteria have developed a unique cell envelope structure that acts as a protective barrier but allows selective passage of nutrients from the external environment and toxic products from the inside of the cell (6). The structure of the Gram-negative cell envelope was revealed in 1969, defining three principal layers: the outer membrane (OM), the peptidoglycan cell wall and the cytoplasmic or inner membrane (IM)(7). Each of these layers possesses distinct features and is discussed in further detail below.

The Outer Membrane

The outer membrane is a characteristic trait of Gram-negative bacteria as it is absent in Gram-positive organisms. It is the first line of defense against extreme environments representing a barrier that blocks entry of toxins and antibiotics and provides mechanical strength to the cell. The OM is a lipid bilayer, where the outer leaflet is composed of lipopolysaccharide (LPS) and the inner leaflet is composed of phospholipids (8). Both inner and outer membrane of Gram-negative bacteria contain phospholipids, however saturated fatty acids and phosphatidylethanolamine are more prevalent in the OM (8). LPS, in turn, consists of three regions: the lipid A glycolipid, the conserved polysaccharide core, and the variable O-antigen formed by repeating units of oligosaccharide (9). The lipopolysaccharide layer plays a significant role in bacterial pathogenicity acting as one of the major virulence factors of Gram-negative bacteria. The lipid A portion of LPS is highly toxic and can trigger a strong immune response via the toll-like receptor pathway in infected hosts (10). Many bacterial species possess an additional extracellular surface-associated polysaccharide layer, that can diffuse into the surrounding creating to a slime layer around the bacterial cell (11). This slime layer provides protection from the environmental threats, antibiotics and desiccation, as well as enables adherence to prosthetic implants, catheters and other smooth surfaces.

There are two classes of proteins that also help compose the outer membrane: lipoproteins, and integral outer membrane proteins (OMPs). Lipoproteins are generally

embedded in the inner leaflet of the OM and perform a structural role by attaching the outer membrane to the underlying peptidoglycan layer (12). Integral OMPs are transmembrane (TM) proteins that adopt a β-barrel conformation which allows them to serve as transports channels (6). These channels, also referred to as porins, are essential for the nutrient uptake and the export of substances such as defence compounds or toxic waste products out of the cell (8). Porins can belong to one of the following classes: non-specific or general porins, substrate-specific channels; energy-dependent or independent (13).

The Inner Membrane

The inner membrane, also referred to as the cytoplasmic membrane, is a phospholipid bilayer that contains integral inner membrane proteins (IMPs), lipoproteins and peripherally attached soluble proteins (6, 14). It serves as a selectively permeable barrier that allows passage of particular ions and molecules, while preventing the movement of other. The cytoplasmic membrane was shown to have the highest level of protein diversity and to be the most complex compartment of the cell envelope (15). Integral or transmembrane proteins comprise α-helical bitopic and polytopic proteins, which span across the membrane once or more than once, respectively (16, 17). Proteins that are attached to only one side of the IM and do not span across it are called monotopic and include peripheral membrane proteins. Peripheral proteins can be attached to the lipid bilayer itself or to integral proteins spanning it, which allows them to act on the surface of the membrane (16, 17). IM proteins perform a wide variety of functions, including solute transport, biogenesis of envelope components, signal transduction, toxic waste disposal, and secretion of proteins and metabolites. Furthermore, complexes in the inner membrane are involved in key processes such as cell division and energy generation via respiratory chains.

The Periplasmic Space

The periplasmic space separates the outer and inner membranes and serves as a site of numerous metabolic reactions and synthesis events, including folding of Sec-secreted proteins. In *E. coli*, it makes up 20–40% of the cell volume (18) and represents an oxidizing microenvironment that is devoid of any known energy-carrying molecules (6, 8, 19). The lack of energy source can become an obstacle for those processes that require the input of energy, for example, biosynthesis at the outer membrane. To overcome this issue, bacteria employ a number of general and specialized chaperones. Together with factors involved in protein folding and trafficking, they assist with the normal function of the periplasm and maintain the cell envelope integrity both during stress and under normal conditions (20).

The peptidoglycan cell wall is a shape-maintaining and osmotic pressure-counteracting structure of the bacterial envelope (21). It composed of two sugar derivatives, N-acetylglucosamine (NAG) and N-acetylmuramic acid (NAM), linked together by a glycosidic bond, which provides rigidity to the cell in the X direction (22). The strength of the peptidoglycan sheet in the Y-direction in conferred by the mesh-like layer of cross-linked amino acids, L-and D-alanine, D-glutamic acid, and either lysine or diaminopimelic acid (DAP). A number of envelope proteins are directly attached to peptidoglycan, including the most abundant protein in *E. coli* Lpp, or Braun's lipoprotein (12), outer membrane protein OmpA, as well as subunits of several envelope-spanning complexes, including the stator element of the flagellar motor complex MotAB (23–25), the Ton molecular motor and the Tol-Pal system. Binding of these proteins to the cell wall from both the inner and the outer membrane sides maintains the size of the periplasmic space, which was shown to be important for signaling processes (26). Perturbations to peptidoglycan layer, such as mutations in penicillin-binding proteins or treatment of cells with drugs affecting peptidoglycan, cause

activation of several envelope stress responses, which in turn adapt by modifying the structure of the cell wall (27, 28).

Protein Transport from the Cytoplasm

All bacterial proteins are synthesised either in the cytoplasm or at the cytoplasmic portion of the inner membrane. After being synthesised, proteins and other macromolecules have to be translocated across the IM into the periplasm or, in the case of phospholipids and LPS, flipped to its outer leaflet (8). The two major pathways associated with protein transport, the Sec pathway (29) and the Tat pathway (30). The Tat pathway is responsible for the export of folded proteins, including those that require cofactor insertion in the cytoplasm (31). The structure and function of the Tat pathway is more comprehensively reviewed in (30, 32)

The Sec translocase is involved in both the secretion of unfolded proteins across, and insertion of integral proteins into the cytoplasmic membrane. The Sec machinery consists of a membrane embedded protein-conducting channel formed by SecY, SecE and SecG components (33), and peripherally associated ATPase SecA, the motor domain that supplies energy for the translocation process (34). There are several accessory membrane proteins, including SecD, SecF and YajC, that can interact with the SecYEG complex, facilitating release of secreted proteins into the periplasm (35–38). In addition, membrane protein insertase YidC assists with the insertion and proper folding of integral inner membrane proteins both dependent and independent from the Sec translocon (39–41). Importantly for this project, in *E. coli* SecYEG and YidC have been shown to be involved in the biogenesis of several electron transport chain (ETC) components, including subunit c and a of the F_1F_0-ATP synthase (F_0c and F_0a), subunit A of cytochrome *o* oxidase (CyoA) and subunit K of NADH dehydrogenase (NuoK)(42–47). For example, NuoK possesses two glutamate residues in its transmembrane segments, E36 and E72, which are required for high rates of quinone activity (48, 49). YidC assists the insertion of these two less hydrophobic, negatively charged segments of the protein

into the membrane (42). In the case of CyoA, YidC assists with insertion of the N-terminus whereas the C-terminus is translocated via the Sec pathway (50).

Envelope-Spanning Protein Complexes

The integrity of the Gram-negative bacterial envelope is partially dependent on the correct assembly and function of the multi-subunit molecular machines spanning the cell envelope. Pili, flagella, RND (resistance-nodulation-division)-type efflux pumps, and a variety of secretion systems are all envelope-localized virulence determinants responsible for adhesion to host cells, bacterium-bacterium interactions, motility, colonization, and immune evasion, and therefore require fine-tuned regulation. The type IV bundle-forming pilus (EPEC), P-pilus (UPEC), toxin co-regulated pilus (*V. cholerae*) and different types of adhesins in *Yersinia* spp. play key role in adhesion to host cells (51–54), whereas flagella acts primarily in locomotion (55). Pili biosynthesis involves both productive pathways, such as the chaperone-usher pathway that assembles P pili (56, 57), and non-productive pathways, in which the absence of a cognate chaperone leads to pilin misfolding (58).

Additionally, successful infection establishment is dependent on the ability of the pathogen to secrete effector proteins. Effector proteins perform diverse functions from remodelling the host cell architecture (59) to preventing or inducing cell death (60–62). Most Gram-negative bacterial pathogens utilize secretion systems, some of which can transport their substrates across both bacterial membranes in a single step, independently of other secretory mechanisms (63, 64). These trans-envelope complexes include type III (T3SS), type IV (T4SS) and type VI (T6SS) secretion systems. T3SS are used by *Pseudomonas*, *Yersinia*, *Shigella* and EHEC to deliver effector proteins into the host cell; functional T3SS are essential for pathogenicity of many bacterial species, including *Yersinia* (65, 66). The T4SS is similar to the T3SS in that it secretes effector proteins, however it is unique in its ability to deliver DNA substrates, and is therefore used for conjugation and uptake or release of DNA (67). For

6

instance, *Neisseria gonorrhoeae* utilizes T4SS to secrete DNA into the extracellular space, which facilitates horizontal gene transfer (68), whereas in *Bordetella pertussis* and *Brucella* spp. it is utilized for toxin secretion and intracellular survival, respectively (69). In addition to delivery of effector proteins to eukaryotic cells, bacteria possessing T6SS are able to establish interbacterial interactions, transporting cell-wall degrading, cell-membrane targeting, and nucleic acid-targeting effectors into the recipient cell (70).

Due to the complex structure of these envelope-spanning complexes, any non-productive assembly pathways or subunit misfolding/mislocalization leads to activation of several partially overlapping envelope stress responses (ESRs). Biogenesis of pili, secretion systems and efflux pumps is assisted with an array of periplasmic protein folding and degrading catalysts that are upregulated in response to envelope perturbations (58).

Quality Control in the Cell Envelope

Protein Folding

As mentioned, the periplasmic space is an oxidizing environment with a redox potential higher than that of the cytoplasm, meaning that molecules in the periplasm will more readily loose electrons (71–74). Both spontaneous (thermodynamically favourable) and assisted folding happens in this compartment of the cell envelope. Two principal catalysts of assisted folding include the DsbA/B pathway, which catalyses oxidative folding of cysteine-containing proteins, and peptidyl-prolyl isomerases or PPIases responsible for *cis-trans* isomerization of peptidyl bonds (74).

Disulfide bonds are introduced into newly translocated proteins by the soluble periplasmic oxidoreductase DsbA (75). DsbA catalyses oxidation of cysteines, forming a covalent S–S bond that links the two amino acid side chains. This reaction occurs via formation of a transient disulfide between DsbA and its substrates, after which DsbA releases in the reduced state (76–78). In order to interact with proteins in the periplasm, DsbA has to be

maintained in an oxidized state *in vivo* (79). Recycling of DsbA back to its oxidized form is performed by the membrane-bound enzyme DsbB, which then delivers electrons to quinones in the respiratory chain (80–82). The electrons are then transferred to the final electron acceptor: molecular oxygen under aerobic conditions and nitrate or fumarate under anaerobic conditions (80). Occasionally proteins, especially those that require formation of non-consecutive disulfide bonds, can be incorrectly oxidized by DsbA and therefore require rearrangement (83). Isomerization of non-native disulfides is performed by the DsbC/D pathway, where DsbC is a soluble homodimeric protein that facilitates proper folding in the periplasm by donating electrons to an incorrectly formed disulfide (80), and DsbD is a membrane-embedded monomeric protein responsible for recycling of DsbC back to its reduced state (80).

The correct folding and structural stability of many secreted and membrane proteins is also dependent on peptidyl prolyl *cis-trans* isomerization performed by PPIases. Prolyl isomerases are highly conserved between different species, however individually they are not essential for viability (84, 85). To date, only four proteins have been classified as periplasmic peptidyl-prolyl *cis-trans* isomerases in *E. coli*, specifically FkpA, PpiA, PpiD and SurA (84). Interestingly, the membrane-anchored PpiD has been described in the literature as a PPIase that facilitates the maturation of β-barrel outer membrane proteins (86). However, recent studies provide evidence that PpiD functions as a chaperone and contributes to the network of other periplasmic chaperones without being specifically involved in OMP maturation (87–89). Furthermore, the role of PpiD in the periplasm appears to be restricted to folding events that take place in close proximity to the inner membrane, as only membrane-anchored PpiD was found to be functional *in vivo* (87).

Proteolysis of inner membrane proteins

Unfolded or misfolded proteins that cannot be rescued by molecular chaperones are targeted for degradation. In the inner membrane, the processes of recognition, recycling and disposal of misassembled or damaged proteins are performed by quality control and proteolytic factors. The term "degradome" is sometimes used to describe the complete set of proteases expressed at any given time by a cell, tissue, or organism (90).

Most intracellular proteolysis is performed by energy-dependent proteases, also known as AAA$^+$ (ATPases associated with diverse cellular activities) proteases (91, 92). FtsH is the only member of the AAA$^+$ superfamily that is membrane-bound and essential in *E. coli* (93); disruption of the *ftsH* operon has only been accomplished in the presence of the suppressor mutation *sfhC21*, which is thought to counterbalance the increased LpxC activity in the absence of FtsH (94, 95). LpxC is a key enzyme in LPS biosynthesis, and its overproduction causes formation of abnormal membrane structures in the periplasm, altering cell morphology (94). Structurally, FtsH is similar to other members of the family and forms a ring-like homo-hexamer with AAA and protease domains located on the cytoplasmic side of the membrane (96–98). *In vivo*, both cytoplasmic and membrane proteins can become targets of FtsH-mediated proteolysis (99–102), although weak unfoldase activity does not allow for efficient degradation of stable proteins (103). FtsH degrades the F$_0a$ subunit of ATP synthase (101, 104) and the SecY subunit of SecYEG translocase (105, 106) when they fail to assemble into a complex with their partner proteins. Interestingly, recognition of membrane proteins by this protease is sequence-independent since it can initiate processive proteolysis at either N or C-termini by recognizing their length but not the exact sequence (107).

The FtsH interaction network includes several integral membrane proteins, including the energy-independent endoprotease HtpX (108) and a pair of periplasmically exposed membrane proteins, HflK and HflC, which together with FtsH form a 'FtsH holoenzyme' (101,

109). HtpX is a zinc-dependent metalloprotease with a cytoplasmic-facing protease domain, however unlike FtsH, HtpX lacks the ATPase domain (110). Acting in membrane homeostasis, HtpX collaborates with FtsH or performs complementary/overlapping functions. For example, it becomes essential when FtsH is absent and, like FtsH, it can degrade SecY (108, 111), although HtpX-dependent cleavage of SecY *in vivo* is significantly less efficient (112). In addition, the activity of FtsH can be modulated by HflK and HflC inner membrane proteins that prevent degradation of membrane-localized substrates by potentially blocking their entry into the proteolytic complex (101, 113). FtsH has been demonstrated to form a complex with HflKC both *in vivo* and *in vitro* though cross-linking and co-immunoprecipitation experiments, and maintain this association within the membrane (97, 113). Overproduction of HflKC was shown to stabilize overproduced SecY protein and has been proposed to inhibit SecY-degrading activity of FtsH protease (113, 114). Interestingly, the translocation and further insertion of HflK and HflC into the inner membrane was found to be strongly dependent on the Sec machinery (115). Another member of the FtsH interactome is the membrane insertase YidC, which was already discussed above. Its contribution to the quality control of membrane biogenesis is supported by the fact that it co-purifies as a part of a large complex with both FtsH and its modulating factors HflK/C (39).

HtrA (high temperature requirement) family of serine proteases are important for maintaining protein homeostasis in extracytoplasmic compartments of the cell (116). One of the protein quality control factor responsible for addressing abnormally folded, unassembled, or oxidatively damaged proteins in the periplasm is DegP. DegP functions primarily in β-barrel OMP biogenesis, and its presence is critical under heat-hock conditions (117). One of the unique features of this protein is that it combines digestive (protease) and remodelling (chaperone) activities. This switch is temperature-dependent: DegP acts as a general molecular chaperone at lower temperatures and possesses proteolytic activity at elevated temperatures

(118). Similar to all above mentioned quality control factors, DegP is a member of FtsH regulatory network, however it does not interact with FtsH directly; it was shown to affect the stability of the HflK subunit of the HflKC modulator complex (115).

The Cpx envelope stress response

Under conditions where the process of membrane protein folding is impaired, bacterial cells react by activating several stress response systems, examples of which in *E. coli* are the σ^E pathway and CpxAR two-component system (119). σ^E pathway has been shown to be predominantly associated with the outer membrane biogenesis. In brief, accumulation of misfolded or inadequately translocated OMPs within the periplasm triggers activation of an alternative RNA polymerase σ factor, encoded by the *rpoE* gene, that globally alters gene expression (120). For a recent review on the σ^E pathway see (121).

Both the CpxAR and σ^E stress response systems detect damage to the cell envelope and alter the expression of many genes that encode for envelope-localized protein folding factors and degrading factors, chaperones and proteases. Similar to how the activity of σ^E system increases in response to the overproduction of various OMPs, the Cpx pathway is stimulated by overproduction of a number of misfolded proteins that accumulate at the inner membrane when over-produced, including the OM lipoprotein, NlpE (122). Despite this apparent overlap, there are a number of signals that activate the CpxAR system but not the σ^E pathway, indicating that these two systems carry out separate functions (123). For instance, σ^E is not activated by NlpE overproduction, and the Cpx system is not induced by misfolded OMPs (124).

CpxAR is a canonical two-component signal transduction system (TCS) that consists of the membrane-localised sensor histidine kinase CpxA and cytoplasmic response regulator CpxR (121, 125, 126)(**Figure 1**). Under non-inducing conditions, the phosphatase activity of CpxA maintains CpxR in a dephosphorylated or inactive state. When the inducing cue is present, CpxA autophosphorylates at a conserved histidine residue and transfers the phosphate

group to CpxR (123). Most of the downstream targets of CpxR transcriptional regulation are genes whose products are involved, either directly or indirectly, in protein folding and degradation in the bacterial envelope (124, 127). In addition, the Cpx regulon includes genes encoding virulence factors, small regulatory RNAs (sRNAs), multidrug efflux systems and peptidoglycan modifying factors (121, 128). Two auxiliary proteins involved in the Cpx regulatory pathway are the periplasmic protein CpxP, one of the most highly expressed members of the Cpx regulon, proposed to inhibit activation of CpxA, and the OM lipoprotein NlpE, which is thought to activate CpxA upon surface adhesion (129–132). The mechanism by which NlpE senses surface adhesion is still under investigation, although it is thought to involve conformational changes in NlpE which bring the lipoprotein in proximity of the CpxA sensing domain (133). Recent studies in EHEC have demonstrated that the sensing of adhesion signals via NlpE was important for the Cpx-mediated expression of virulence genes during infection, specifically type III secretion system and flagella (134). Other mechanisms have been proposed for NlpE, including those where it acts as a sensor for monitoring stress related to lipoprotein trafficking and periplasmic redox state (135). Lipoprotein processing issues result in mislocalization and accumulation of NlpE in the IM, which is sensed by CpxA (136). In addition, NlpE can act as a sensor for redox perturbations, and activate Cpx response when one of its two pairs of cysteines is not oxidized, and the C-terminal disulfide bond is not formed (135).

The Cpx system is triggered by a variety of signals, including alkaline pH, aminoglycoside antibiotics, NlpE overexpression, aberrant expression of P-pilus subunits, mutation of the IM protease FtsH, depletion of membrane insertase YidC and changes to peptidoglycan composition (28, 58, 110, 129, 131, 137–141). These activating cues are related to potentially lethal accumulation of misfolded or mislocalized proteins at the bacterial envelope. To restore the integrity of the envelope, the Cpx response upregulates proteolytic

factors and periplasmic protein folding factors, including the disulfide bond oxidoreductase DsbA, the peptidyl-prolyl isomerase PpiA, the chaperones Spy and CpxP (127, 129, 142, 143), and the protease/chaperone DegP (142, 144). For instance, non-productive assembly of P pili results in the activation of the Cpx pathway and subsequent upregulation of DegP that degrades misfolded pilin subunits (58). Additionally, as an adaptation to stresses that lead to protein misfolding, the Cpx pathway directly represses transcription of high molecular weight protein complexes (121, 128, 145)**(Figure 1)**.

In order to maintain membrane homeostasis and to optimize gene expression under stressful conditions, the Cpx and other stress responses rely on the activity of several small regulatory RNAs (sRNAs) which are discussed in greater detail below. Many of them participate in feedback and feed-forward loops, which constitute global regulatory networks, allowing bacteria to quickly respond to environmental changes (146).

Small Regulatory RNAs

Besides the aforementioned protein folding and degrading factors, the Cpx response both directly and indirectly regulates the expression of several sRNAs, including CyaR, RprA, OmrA, and OmrB, as well as is regulated by RprA sRNA (147). Small regulatory RNAs are widely distributed among bacteria, where their activity causes changes in translation initiation, RNA stability, and/or transcription elongation. Numerous sRNAs have been discovered and functionally characterized in the past 20 years revealing an extensive network of post-transcriptional control spanning all branches of bacterial physiology. These single-stranded RNA molecules are usually 50-200 nucleotides in length, target specific messenger RNA (mRNA) molecules and thus are utilized for gene regulation (148). sRNAs possess highly conserved 'seed' regions, that are typically 7-12 bp in length and serve to recognize mRNA targets (149, 150).

sRNAs can negatively affect translation and stability of their mRNA targets. Binding of sRNAs in the translation initiation region (TIR) suppresses protein synthesis due to direct competition between the initiating 30S ribosomal subunits and the inhibitory sRNAs paired with the Shine-Dalgarno (SD) sequence. Furthermore, sRNAs can promote degradation of transcripts by RNase enzymes (151) or cause premature transcription termination in a Rho-dependent or independent (intrinsic) manner (152). In contrast, sRNAs can also positively regulate mRNA expression by remodeling inhibitory secondary structures within a target molecule, or by blocking access of negative regulators such as RNases or Rho transcription termination factors (151). Interestingly, there is a class of RNA molecules involved in regulation of the sRNAs themselves. These "sponge" RNAs form RNA-RNA interactions with their targets and promote degradation of the sRNA itself or of the sponge RNA-sRNA complex (153–156).

In *E. coli*, the association of sRNAs with their target mRNAs often requires the assistance of RNA chaperones Hfq or ProQ, which stabilize sRNAs and facilitate the RNA-RNA pairing (149, 157–162). Hfq possesses a characteristic ring architecture, which offers three sites for potential interaction with RNA, the proximal and distal faces of the ring, as well as the lateral rim (149, 151). Interestingly, Hfq has also been reported to function in collaboration with an endoribonuclease RNase E, the primary enzyme of general mRNA turnover (163). A more detailed review on sRNAs in bacteria can be found in (164).

The majority of sRNAs are expressed in response to environmental conditions to maintain cellular homeostasis. For example, one of the well-characterized Hfq-associated sRNA RyhB is expressed under iron (Fe) starvation and negatively regulates non-essential Fe-dependent proteins in order to preserve sufficient intracellular Fe for survival (165). The *sdhCDAB* polycistronic mRNA encoding the succinate dehydrogenase enzyme of the tricarboxylic acid (TCA) cycle was one of the first identified targets of RyhB post-

transcriptional regulation (165). Other sRNAs acting in envelope homeostasis include Spot 42 (also known as Spf), MicA, RybB and CpxQ. Spot 42 plays a role in catabolite repression and its targets are involved in many aspects of cellular metabolism (166, 167) ,whereas both MicA and RybB are expressed following membrane stress and are known to repress the synthesis of several major OMPs (168–175).

One of the most relevant RNA-based control mechanisms for this project is the activity of the CpxQ sRNA, first described in 2016 (176). CpxQ is produced via RNase E-mediated cleavage of the 3' untranslated region (UTR) of the *cpxP* mRNA and constitutes the most conserved region of the entire *cpxP* gene (176). CpxQ is an Hfq-associated sRNA that has been found to inhibit the production of several IM- and periplasm-localized proteins, including a sodium-proton antiporter NhaB, glucose-1-phosphotase Agp, and the periplasmic chaperones Skp and CpxP (176, 177). Interestingly, CpxQ was also proposed to regulate bacterial adhesion through diminishing expression of the major fimbrin subunit of type 1 pilus *fimA* (176), and to repress the expression of cyclopropane fatty acid synthase (encoded by *cfa*)(178).

The abovementioned targets of CpxQ have been implicated in generating envelope stress when overproduced, either by damaging the membrane potential in the case of NhaB (176), or by aberrant insertion of OM proteins into the IM in the case of Skp (177). In *Salmonella*, bacteria lacking CpxQ demonstrated increased sensitivity to the protonophore carbonyl cyanide *m*-chlorophenylhydrazone (CCCP), a reagent that disrupts the proton motive force (PMF) at the IM (177). In contrast, treatment with CCCP did not trigger the Cpx response and hence CpxQ activation in *E. coli* (129, 179). Intriguingly, a recent study uncovered a number of novel sRNA base-pairing interactions utilizing the UV cross-linking, ligation and sequencing of hybrids (CLASH) method, expanding the regulatory network of 3'UTR-derived sRNAs (180). Moreover, it has been demonstrated that CpxQ along with RybB sRNA are the primary targets of the FtsO sponge RNA, which when overexpressed, decreases their cellular

levels (181). Even though little is known about the role of CpxQ in envelope biogenesis and further studies are required, a growing body of evidence points to a significant role of sRNAs in stress alleviation.

The Electron Transport Chain of *Escherichia coli*

The ETC incorporates some of the largest multiprotein complexes in the *E. coli* IM, making them a primary target of Cpx regulation (179). *E. coli* is a facultative anaerobic microorganism which generates energy by aerobic respiration if oxygen is present but is capable of switching to fermentation or anaerobic respiration if oxygen is limited. The electron transport chain complexes convert the energy of reducing equivalents, such as NADH or FADH$_2$, into a proton electrochemical gradient across the membrane. This electrochemical gradient drives ATP synthesis via ATP synthase or can be used directly for other energy consuming processes in the cell, including active transport and flagellar motion (182–187). The ETC is localized to the inner membrane and consists of several major respiratory complexes including NADH dehydrogenase I and II (NDH-I and NDH-II, respectively), succinate dehydrogenase (SDH), cytochrome *bo₃*, cytochrome *bd*-I, and cytochrome *bd*-II **(Figure 2)**.

The first steps of electron transport are catalyzed by NADH dehydrogenase (NDH-I), the largest complex of the ETC (188), and the entry point for electrons carried by NADH (189, 190)**(Figure 3A)**. In *E. coli*, the *nuo* operon contains 13 genes, *nuoA-N*, where *nuoC* encodes a fused version of NuoC and NuoD subunits (184, 191, 192). NDH-I is an L-shaped multisubunit structure composed of a hydrophobic membrane arm, protruding into the lipid bilayer, and a hydrophilic peripheral arm that extends into the cytoplasm (193–195). The processes of proton translocation and quinone binding take place in the membrane arm consisting of NuoA, H, and J-N, whereas NADH oxidation is the function of the peripheral arm comprising NuoB, CD, E, F, G, and I subunits (194). The catalytic arm of the NDH-I complex contains the redox groups, including one flavin mononucleotide (FMN) and eight or

nine iron-sulfur (Fe-S) clusters that are required for electron transfer due to their ability to access various redox states (186, 196). The free energy gained from the process of electron transfer (−0.42 eV per electron) between NADH and quinone is utilized by NDH-I to pump up to four protons across the bacterial membrane (186).

Succinate dehydrogenase (SDH) is a unique membrane-bound enzyme that is common between the ETC and the TCA cycle (197)**(Figure 3B)**. Within the TCA cycle, SDH oxidizes succinate to fumarate sequestering two electrons, which are then used for the reduction of ubiquinone in the membrane (198). It is composed of four nonidentical subunits encoded by the *sdhCDAB* operon, where SdhA and SdhB are the cytoplasmic catalytic subunits which contain the flavin adenine dinucleotide (FAD) and Fe-S cluster cofactors, respectively. SdhC and SdhD compose the membrane-integral part of the enzyme and contain the ubiquinone binding site and the heme b cofactor (184, 198, 199). The absence of either SdhC or SdhD structural components leads to unstable SDH activity in the cytoplasm as well as perturbation to ubiquinone reduction at the IM (200).

Thesis objectives

While a detailed mechanism of how electrons are transported through the respiratory complexes, and how this process is coupled to energy production has been revealed, the biogenesis mechanism of these multiprotein complexes is still under investigation. Transcripts encoding complexes of the ETC have been identified in all transcriptomic studies of the Cpx response to date, nevertheless the quality control of respiratory proteins at the inner membrane of *E. coli* is one of the least characterized parts of the whole Cpx regulatory network. The aim of this project was to further study the association between the Cpx envelope stress response and the electron transport chain, and identify the Cpx-regulated factors involved in post-transcriptional and post-translational control of the ETC complexes. The specific objectives were:

1. Regulation of the succinate dehydrogenase respiratory complex:

    a. To confirm the results of the microarray experiments suggesting that activation of the Cpx response downregulated the expression of genes encoding SDH

    b. To determine whether inactivation or activation of the Cpx response affects the performance of the SDH enzyme complex

2. Quality control of the NADH dehydrogenase I complex:

    a. To determine whether the Cpx response regulates NDH-I at the post-translational level

    b. To identify Cpx-regulated protein folding and degrading factors involved in the protein turnover of NDH-I

3. Effects of increased respiratory demand on the Cpx pathway activation:

    a. To confirm the generation of additional envelope stress by the respiratory complexes

4. Effects of the CpxQ sRNA overexpression on the stability of respiratory chain mRNAs

    a. To determine if the Cpx stress response non-coding arm regulates the ETC complexes at a post-transcriptional level

    b. To determine the mechanism by which CpxQ sRNA regulates the ETC transcripts

Introductory Figures
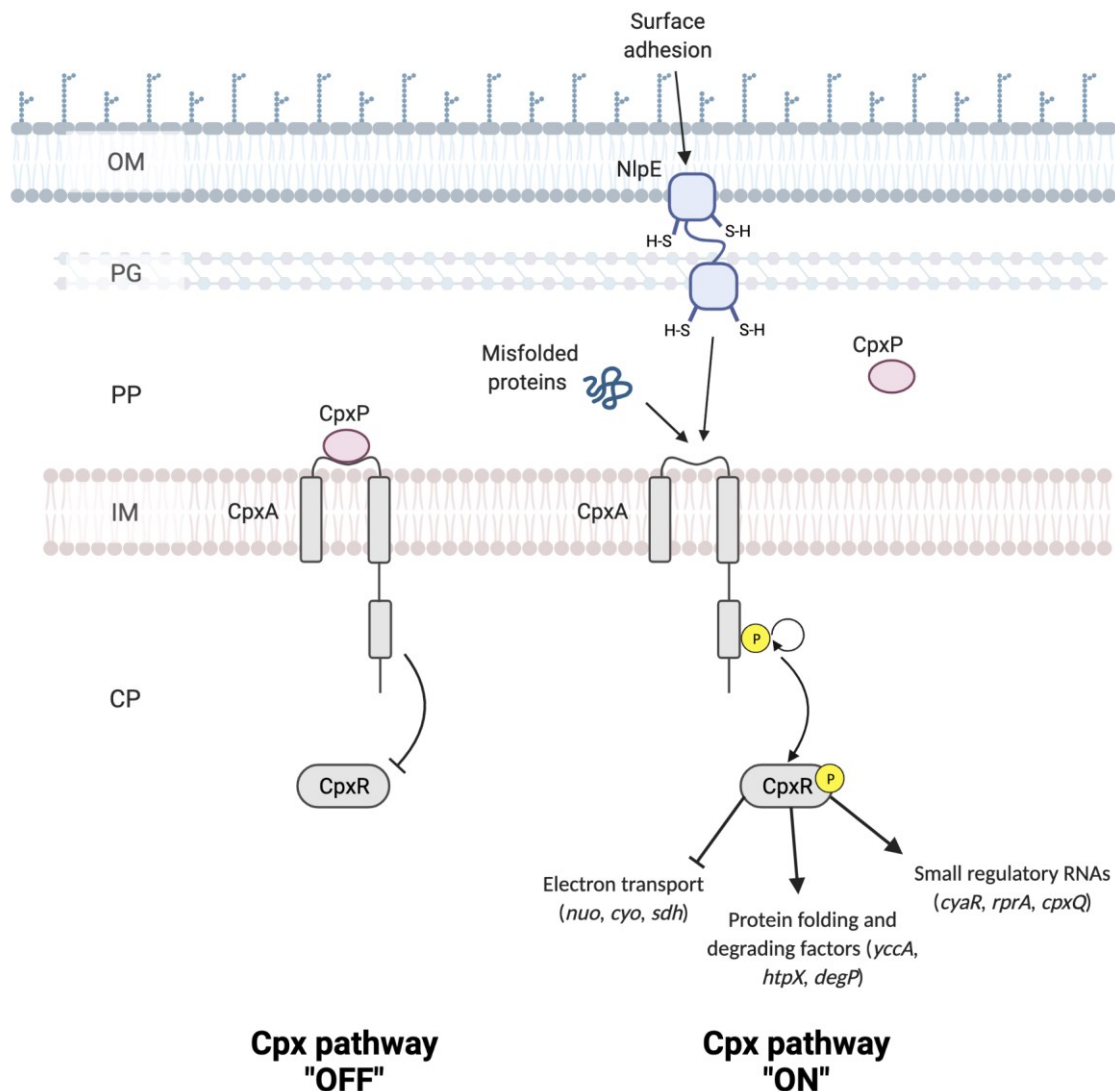
Figure 1. The Cpx envelope stress response. The Cpx pathway is a canonical two-component system comprised of the sensor histidine kinase CpxA and the response regulator CpxR. Under non-inducing conditions, the phosphatase activity of CpxA keeps CpxR in an unphosphorylated or inactive state. Under inducing conditions, CpxA autophosphorylates using ATP as its phosphoryl donor, and transfers the phosphate group to CpxR. Other regulatory factors include the periplasmic protein CpxP, one of the most highly expressed members of the Cpx regulon, suggested to inhibit activation of CpxA; and the OM lipoprotein NlpE which is thought to activate CpxA upon sensing stresses associated with lipoprotein

trafficking defects, changes in periplasmic redox state and surface adhesion. The Cpx response is triggered by a variety of signals, including alkaline pH, aminoglycoside antibiotics, overexpression of NlpE and accumulation of misfolded proteins in the envelope. CpxR directly regulates the transcription of multiple targets, including envelope-localized multi-protein complexes, quality control factors and small regulatory RNAs. This list is not exhaustive of the Cpx regulon. OM, outer membrane; PP, periplasm; PG, peptidoglycan; IM, inner membrane; CP, cytoplasm; P, phosphate. This figure is adapted from (121).
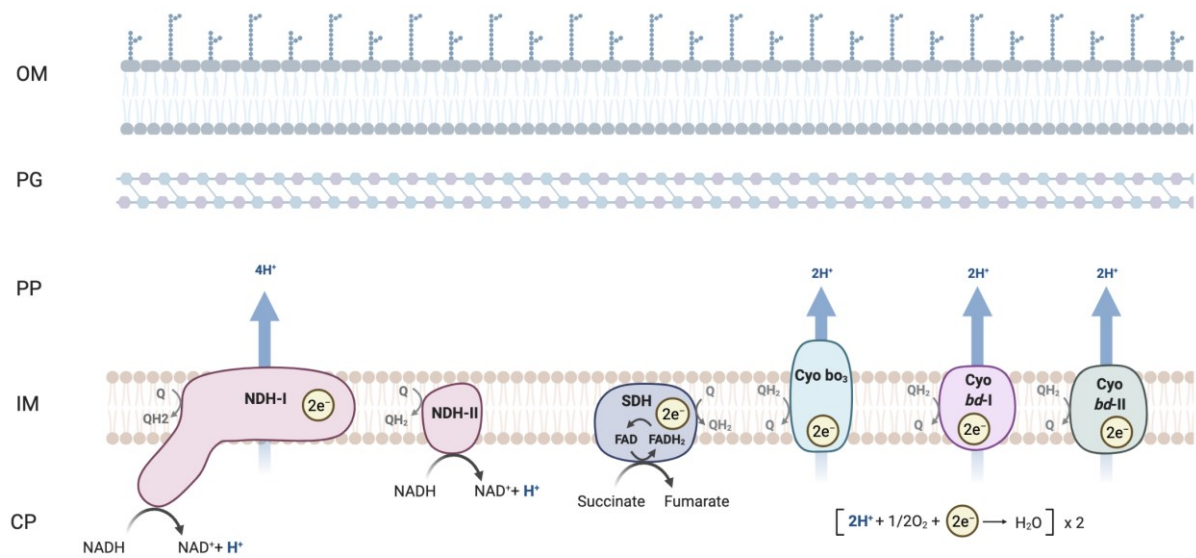
Figure 2. The Electron Transport Chain of *E. coli*. The ETC is composed of primary dehydrogenases and terminal oxidases that are connected by electron carriers known as quinones. General topology of the following complexes is shown: NDH-I, NADH dehydrogenase I; NDH-II, NADH dehydrogenase II; SDH, succinate dehydrogenase; cytochrome *bo₃*, Cyo *bo₃*; cytochrome *bd*-I and *bd*-II, Cyo *bd*-I and Cyo *bd*-II. Q, quinone; QH₂, quinol; H⁺, proton; NAD, nicotinamide adenine dinucleotide; FAD, flavin adenine dinucleotide; H₂O, water; O₂, molecular oxygen.

A

B
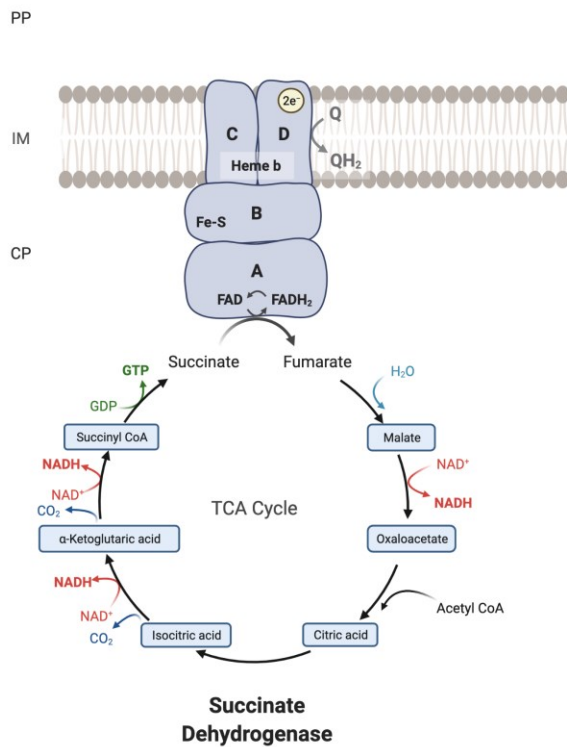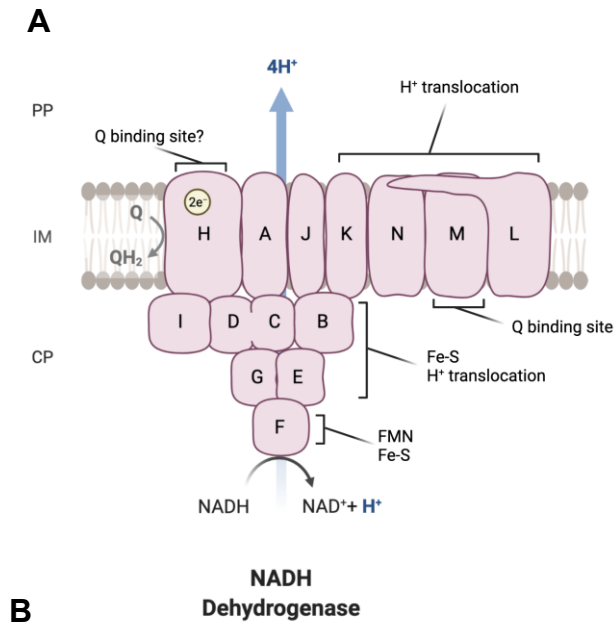
Figure 3. Simplified structure of the NADH dehydrogenase I (NDH-I) and succinate dehydrogenase (SDH) complexes. (A) NDH-I is an L-shaped, redox-driven proton-pumping protein complex, that consists of 13 subunits, where subunits NuoC and NuoD are fused. Peripheral arm of NDH-I is comprised by NuoF, G, E, I, CD and B subunits and contains 8-9 Fe-S bridges facilitating electron transfer between NADH and quinone. Subunit NuoF is

thought to contain one flavin mononucleotide molecule (FMN) that functions as an e^- carrier. The membrane arm primarily acts in H^+ translocation, ensures structural integrity of the complex, and is thought to contain the quinone binding site either in the NuoM or NuoH subunits. **(B)** SDH is a membrane-bound enzyme participating in both the respiration and the TCA cycle, where is oxidizes succinate to fumarate. It consists of four subunits: SdhA contains FAD cofactor, SdhB contains three Fe-S clusters for electron transfer between FAD and the ubiquinone, and the membrane anchor subunits SdhC and D form cytochrome b_{556} and interact with ubiquinone. Q, quinone; QH_2, quinol; H^+, proton; NAD, nicotinamide adenine dinucleotide; FAD, flavin adenine dinucleotide; CO_2, carbon dioxide; H_2O, water; GDP, guanosine diphosphate; GTP, guanosine triphosphate; Fe-S, iron-sulfur bridge. Information used to draw the structures was taken from (184, 186, 195, 201).

MATERIALS AND METHODS

Bacterial strains and growth conditions. All bacterial strains and plasmids used in this study are listed in Table S1. Cultures were routinely grown and maintained in LB broth or M9 minimal medium (Difco) at 37°C with shaking at 225 rpm, with the exception of strains bearing the *cpxA24* mutation, which were grown at 30°C in the presence of amikacin (3μg/ml) to prevent accumulation of suppressors as previously described (130). Isopropyl-β-D-thiogalactopyranoside (IPTG, Invitrogen) was added to a concentration of 0.1mM to induce gene expression from pCA24N and pMPM-K3 based vectors. 0.2% arabinose concentration was used to induce the expression of CpxQ from pBAD-CpxQ vector for 10 minutes. Antibiotics (Sigma) were added as necessary at the following concentrations: chloramphenicol (Cam), 25μg/mL; kanamycin (Kan), 30μg/mL or 50μg/mL; ampicillin (Amp), 100μg/mL; spectinomycin (Spc), 25 μg/ml.

Strain and plasmid construction. All bacterial strains and plasmids used in this study are listed in **Table 1**. All BW25113 mutants were taken from the Keio collection (202). A Δ*cpxR* knockout mutant was generated using P1 transduction to move the desired mutant allele from the Keio collection (202) into wildtype MC4100 as previously described (203). The inducible pCA24N-based plasmids used in this study were obtained from the ASKA collection (204). Transcriptional luminescent reporters containing the promoter regions of *cpxP* and *nuoA* were constructed as previously described (179, 205, 206). The p*sdhC*::*lux* reporter was constructed similarly. Briefly, the promoter region of *sdhC* gene was amplified by PCR, using PsdhCFwdCln and PsdhCRevCln primers (**Table 2**). Purified PCR products and the pJW15 vector (207) were digested with EcoRI and BamHI (Invitrogen), and the insert was ligated upstream of the *luxCDABE* operon in the pJW15 plasmid. Correct insertion of the promoter sequence was verified by PCR and sequencing using pNLP10F and pNLP10R primers (**Table 2**).

For the construction of pTrc-*nlpE* vector, *nlpE* was amplified via PCR with recombinant Taq polymerase (Invitrogen) using nlpE_NcoI_F and nlpE_WT_HindIII_R primers (**Table 2**). PCR products were purified using a QIAGEN QIAQuick PCR purification kit according to the manufacturers protocol. Amplified *nlpE* was digested along with purified pTrc99A using Fast Digest EcoRI and HindIII (Thermo Scientific). Digests were purified using the aforementioned PCR purification kit and were then ligated together using T4 DNA ligase. Ligations were then transformed into One Shot TOP10 chemically competent cells (Thermo Fisher). Correct insertion of the *nlpE* sequence was verified by PCR and sequencing using pTrc99A_F and pTrc99A_R primers (**Table 2**).

The pMPM-NuoA-3×FLAG plasmid was constructed by amplifying *nuoA* from the E2348/69 chromosome via PCR using primers nuoAFLAGFwd and nuoAFLAGrev (**Table 2**). Primer nuoAFLAGrev contains the nucleotide sequence to insert a triple FLAG-tag directly upstream of the *nuoA* stop codon. PCR was performed using high-fidelity phusion DNA polymerase (ThermoFisher) according to the manufacturers protocol with the addition of 10% betaine. The DNA band corresponding to *nuoA*-3×FLAG DNA was gel extracted and cleaned using the GeneJet gel purification kit (Fermentas). Both *nuoA*-3×FLAG and pMPM-K3 DNA were digested with the HindIII and XbaI restriction endonucleases (Invitrogen) according to the manufacturers protocol. *nuoA*-3×FLAG DNA was then ligated downstream of an IPTG inducible P*lac* promoter in the pMPM-K3 vector and transformed into One Shot TOP10 chemically competent *E. coli* (Invitrogen) as per the manufacturer's protocol. PCR and DNA sequencing were used to confirm the presence of *nuoA*-3×FLAG fragment within pMPM-K3 using M13F and M13R primers (**Table 2**). All DNA sequencing was performed by The University of Alberta Molecular Biology Services Unit (MBSU). All plasmids in this study were transformed into *E. coli* strains via chemical competency (203).

For the construction of pBAD-CpxQ vector, *cpxQ* containing EcoRI and XBaI restriction sites was synthesized by Integrated DNA Technologies (IDT), where the entire *cpxQ* sequence was cloned into the pIDTSMART-AMP high-copy number vector (sequences are listed in **Table 2**). Both pIDTSMART-AMP and pBAD18 vectors were digested using EcoRI and XBaI restriction endonucleases (Invitrogen) according to the manufacturers protocol. Digested pIDTSMART-AMP was run on a 1% agarose gel, and the band corresponding to *cpxQ* was gel extracted and purified using a QIAquick Gel Extraction Kit according to the manufacturer's instructions. *cpxQ* DNA was then ligated downstream of an arabinose-inducible P*ara* promoter in the pBAD18 vector. DNA sequencing was used to confirm the presence of the *cpxQ* fragment within pBAD18 using pBAD_fwd and pBAD_rev primers (**Table 2**).

The plasmid pMPM-*sdhC*-6×His was constructed in order to create a variant of SdhC that was six-His tagged at its C-terminus. *sdhC* was amplified from the MC4100 chromosome via PCR using primers sdhC_FW_pMPM and sdhC_RV_pMPM (**Table 2**). Primer sdhC_FW_pMPM binds 46 bp upstream of the *sdhC* start codon to include the putative SdhC Shine-Dalgarno sequence. Primer sdhC_RV_pMPM contains the nucleotide sequence to insert a six-His tag directly upstream of the *sdhC* stop codon. PCR was performed using high-fidelity Phusion DNA polymerase (ThermoFisher) according to the manufacturer's protocol with the addition of 10% betaine. Two-step PCR was performed with the following conditions: denaturation stage, 98°C for 10 seconds; annealing stage, 72°C for 30 seconds; final extension stage, 72°C for 10 minutes. PCR products were purified using a QIAGEN QIAQuick PCR purification kit according to the manufacturer's protocol. Amplified *sdhC* was digested along with purified pMPM-K3 using Fast Digest EcoRI and XbaI (Thermo Scientific). Digests were purified using the aforementioned PCR purification kit and were then ligated together using T4 DNA ligase. Ligations were then transformed into One Shot TOP10 chemically competent

cells (Thermo Fisher). Correct insertion of the *sdhC*-6×His sequence was verified by PCR and sequencing using M13F and M13R primers (**Table 2**).

Luminescence assay. Strains containing p*cpxP*::*lux*, p*sdhC*::*lux* or p*nuoA*::*lux* reporter plasmids were grown overnight in LB broth with shaking at 37˚C. Cells were pelleted by centrifugation and washed twice with phosphate-buffered saline (PBS). The cell density was standardized to OD_{600} 1.0, pelleted and resuspended in 1mL of 1×PBS. Standardized cultures were serially diluted 10-fold and 10µL of each dilution was spotted onto M9 minimal agar containing 0.4% glucose, malic acid or succinic acid (Sigma). Glucose-succinate gradient agar plates were created by pouring M9 containing 0.4% glucose into an angled plate. The layer was allowed to solidify in the inclined position and the second portion of agar containing 0.4% succinic acid was poured into the plate, placed on a level surface and allowed to solidify (208). Agar pH was adjusted to 7.0 with sodium hydroxide. Bacteria were grown for 24-48 h at 37°C statically. Luminescence was determined by imaging the light produced by strains using the UVP Colony Doc-It Imaging Station (Biorad). Luminescence was quantified using Fiji (ImageJ).

For the assay performed in liquid medium, bacteria were grown overnight as described above, subcultured at a dilution factor of 1:100 into 5 ml of fresh LB broth and incubated for 2 h at 37°C with aeration. 200µL of each subculture was aliquoted into a black-bottomed 96-well plate, and luminescence in counts per second (CPS) and OD_{600} were measured every 1 h for 7h post-subculture using a PerkinElmer VICTOR™ X3 multilabel reader. Luminescence and OD_{600} values measured from a blank well containing uncultured LB were subtracted from each sample. CPS was standardized to the OD_{600} to correct for differences in cell numbers between samples. All experiments contained three technical replicates and were carried out three times.

Western blot analysis. Samples used for Western blot analysis were prepared by diluting overnight cultures 1:100 into 25 ml fresh LB containing appropriate concentrations of antibiotics. Bacteria were grown at 37°C with shaking to an OD_{600} of ~ 0.35. IPTG was added to a concentration of 0.1mM and bacteria were grown for an additional 30 minutes as before. 2 × 1mL samples were collected. Cells were pelleted by centrifugation at 21,130 × g for 1 minute. One sample was resuspended in 50µL 2× Laemmli sample buffer (Sigma) and the other sample was resuspended in 50µL 1× PBS. Protein concentration was determined from the sample resuspended in phosphate-buffered saline using the Pierce BCA protein assay kit (ThermoFisher) according to the manufacturers' protocol. Samples resuspended in 50µL 2× Laemmli sample buffer were denatured by boiling for 5 minutes. Sample volumes were standardized according to their determined protein concentrations and separated on a 12% SDS gel at 110V for 1.5 hours in Tris-glycine running buffer (10% SDS, 250mM Tris, 1.2M glycine). Proteins were transferred onto a nitrocellulose membrane via the trans-blot semi-dry transfer system (Bio-Rad) at 15V for 22 minutes using semi-dry Towbin transfer buffer (78mM glycine, 1.3mM SDS, 20% methanol). Membranes were blocked in 5% MTS (2.5% skim milk powder, 154mM NaCl, 1mM Tris) or 2% BSA (154mM NaCl, 1mM Tris, 1% Tween 20, 2% bovine serum albumin) for 1 hour at room temperature with shaking at 10 rpm. Primary α-FLAG (Sigma, BioLegend), α-PhoA (Abcam) and α-RNAPα (BioLegend) antibodies were diluted by a factor of 1:5000 into 5% MTS or 2% BSA. Membranes were incubated with the primary antibody for 1 hour at either room temperature with shaking at approximately 10 rpm or overnight at 4°C with rocking. Following incubation with the primary antibody, membranes were washed for 5 minutes in wash solution (154mM NaCl, 1mM Tris, 1% Tween 20) four times. Alkaline-phosphatase (AP) anti-rabbit secondary antibodies (Sigma) were diluted at a factor of 1:10000 in 5% MTS and were used to detect the α-PhoA (Abcam) and α-FLAG (Sigma) primary antibodies. IRDye®680RD Goat anti-Mouse 925-68070 and IRDye®800CW

Goat anti-Rabbit 925-32211 secondary antibodies (LI-COR) were diluted at a factor of 1:15000 in 5% MTS and were used to detect the α-RNAPα (BioLegend) and α-FLAG (BioLegend) primary antibodies, respectively.

Membranes were then incubated with the secondary antibody for 1 hour at room temperature with shaking at approximately 10 rpm. Membranes were washed following incubation with the secondary antibody as before. Proteins from the membranes incubated with AP secondary antibodies were detected using the Immun-Star alkaline phosphatase chemiluminescence kit (Bio-Rad). All membranes were imaged with the Bio-Rad ChemiDoc MP imaging system. Quantification of each band compared to the wildtype was performed using band intensity analysis in Fiji (ImageJ). Experiments were performed in biological triplicates, and a representative blot is shown in each case.

Protein Stability Assay. Bacteria were grown overnight in 5mL LB at 37°C with shaking. The following day, bacteria were subcultured at a 1:100 dilution into 25mL fresh LB and grown at 37°C with shaking to an $OD_{600} \sim 0.5$. IPTG was then added to a final concentration of 0.1mM and bacteria were grown to an OD_{600} of 1.0. 1mL samples were collected and cells were pelleted by centrifugation at $21,130 \times g$ for 1 minute. After the supernatant was removed, cells were resuspended in 50μL 2×Laemmli sample buffer (Sigma). Immediately after the sample was removed, the protein synthesis inhibitor chloramphenicol was added to the remaining culture at a concentration of 100μg/mL. The culture was incubated at 37°C and shaken at 225 rpm. 1mL of culture was collected at 0 (before the addition of chloramphenicol), 1, 5, 10, 20, 30, 45, 90, and 120 minute(s) after the addition of chloramphenicol. Sample collection at each timepoint was performed as described above. 10μL of each sample was loaded onto a 12% SDS polyacrylamide gel. Incubation with primary and secondary antibodies, detection and band quantification were performed as described above. Each experiment was repeated three times, and a representative blot is shown in each case.

Succinate dehydrogenase activity assay. Succinate dehydrogenase activity was measured using a kit (Abcam). Samples were prepared following the manufacturer's protocol by diluting overnight cultures 1:50 into 5mL fresh LB and growing them to OD_{600} ~0.5 at 37°C with shaking. 1 mL of culture was taken, pelleted by centrifugation, washed with 1×PBS and pelleted again. Cultures were then standardized to the same optical density OD_{600} of 1.0 in the final volume of 1mL by adding appropriate volume of 1× PBS, pelleted, and resuspended in 200µL of ice-cold SDH Assay Buffer (Abcam). Cell lysis was performed by sonication. Samples were centrifuged at 10,000 × g for 5 minutes and the supernatant was transferred into a fresh tube. 50µL of each sample was loaded into a 96-well plate, and 50µL of SDH reaction mix containing the SDH substrate mix, and the probe (Abcam) was added to them. Absorbance at 600nm was measured for 30 minutes at 25°C in kinetic mode using the Cytation5™ Cell Imaging Multi-Mode Reader (BioTek). The succinate dehydrogenase activity of the samples was calculated according to the manufacturers' directions. Data is representative of the means and standard deviations of three biological replicates.

Minimal media growth assays. Wildtype BW25113 or knockout mutants were grown overnight in 2mL LB at 37°C with shaking. The following day, cells were pelleted by centrifugation and washed twice with phosphate-buffered saline. The density was standardized to OD_{600} 1.0 by suspending an appropriate volume of cells in 1 ml of 1×PBS. 20µL of each sample was loaded into a 96-well plate, each well containing 180µL of either 0.4% glucose (Sigma), 0.4% malic acid (Sigma) or 0.4% succinic acid (Sigma) M9 minimal medium (Difco), pH 7.0. The plate was incubated in the Cytation5™ Cell Imaging Multi-Mode Reader with 330 rpm shaking at 37°C for 48 hours.

RNA isolation and cDNA synthesis. RNA was isolated from 25mL LB subcultures carrying the appropriate antibiotics that had been inoculated with a 1:50 dilution of an overnight culture. Strains were grown to an early log stage (OD_{600} of ~0.35 to 0.4) at 37°C with shaking and

grown for 10 more minutes either with or without 0.2% arabinose. 3 mL samples were harvested and RNA was isolated using a MasterPure RNA purification kit as described by the manufacturer (Epicentre Biotechnologies). Isolated RNA was resuspended in 35μL of nuclease-free water (IDT). Quality control of the extracted RNA was determined using an Agilent 2100 Bioanalyzer System at the University of Alberta Molecular Biology Service Unit (MBSU). During quality control analysis, the sample components are electrophoretically separated and their components are detected by fluorescence.

For cDNA synthesis, RNA concentrations were standardized to 500 ng/μL, and 1μg of RNA was mixed with 3.3μL of 300ng/μl of random primers (Invitrogen), 1μL each of all deoxynucleoside triphosphates (dNTPs)(10 mM; Invitrogen), and nuclease-free water to a final volume of 10μL. The random primers and RNA were allowed to anneal (70°C for 10 min and 25°C for 10 min). After the annealing step, the RNA-primer hybridization mixture was added to 4μL of 5× 1st Strand Buffer, 2μL of 100mM DTT, 1.5μL of 20U/μl SUPERase•In (optional), 2.5μL of 200U/μl SuperScript II, and nuclease-free water to a final volume of 20μL. The mixture for cDNA synthesis was incubated at 25°C for 10 min, 37°C for 1 h, 42°C for 1 h, and 70°C for 10 min.

qPCR. The qPCR primers were designed to amplify approximately 75 nucleotides in the last 500bp of each gene of interest and are listed in **Table 2**. qPCR was performed with a 96-well microtiter plate containing a 10μl reaction mixture of the 2× QPCR Mastermix (*Dynamite*), 2.5μl of a 3.2 μM stock solution of each primer and 2.5μl of a 500ng/μl cDNA template. The 2× QPCR Mastermix (*Dynamite*) used in this study is a proprietary mix developed, and distributed by the Molecular Biology Service Unit (MBSU), in the Department of Biological Science at the University of Alberta, Edmonton, Alberta, Canada. It contains Tris (pH 8.3), KCl, $MgCl_2$, glycerol, Tween20, DMSO, dNTPs, ROX as a normalizing dye, SYBR Green (Molecular Probes) as the detection dye, and an antibody inhibited Taq polymerase. The qPCR

was carried out by incubation at 95°C for 15 s, followed by 60°C for 1 min. This cycle was repeated for a total of 40 times, using a 7500 Fast Real-Time PCR system (Applied Biosystems). Relative amounts of PCR product were determined by monitoring the number of cycles required to reach a threshold level of fluorescence (cycle threshold [C_T]) for each gene and subtracting this number from the C_T value for an endogenous control gene known not to be Cpx regulated. We used the *gyrA* gene for this purpose. The resulting delta CTs ($\Delta C_T{}^s$) for given genes were compared between the wildtype and strains containing a CpxQ overexpression vector to obtain delta-delta C_T values ($^{\Delta\Delta}C_T{}^s$), which represented the change in gene expression between different strains.

RESULTS

Regulation of the SDH complex by the Cpx response. Recent studies demonstrated that the expression and activity of NDH-I and cytochrome bo_3 complexes is regulated by the Cpx envelope stress response in EPEC (179). In addition, significant Cpx-dependent downregulation of genes encoding the succinate dehydrogenase complex was observed in a large microarray dataset, however the mechanism of regulation has not been revealed (145). To investigate the impact of the Cpx two-component system on the SDH, we grew strains carrying either the vector control or a reporter plasmid, in which 500 bp upstream of the *sdhCDAB* operon were fused to the *luxCDABE* gene cluster, in liquid LB medium aerobically for 24 hours. Luminescence activity of the *sdhC*::*lux* reporter in the presence or absence of the Cpx pathway was measured every hour until the stationary phase was reached. The luminescence activity produced by the *cpxP*::*lux* reporter gene was used as a positive control, since CpxP is one of the most upregulated members of the Cpx regulon (206). In agreement with previous observations, the expression of the *cpxP*::*lux* reporter in the wildtype BW25113 showed large increases in luminescence compared to that of the *cpxA* null background at every stage of growth (**Figure 1A**).

Along with *cpxP*, we assayed the activity of the *nuoA*::*lux* reporter and were able to validate its Cpx-dependent downregulation, reported in the past (**Figure 1B**)(179). Loss of Cpx response resulted in a ~2-fold increase in the *nuoA*::*lux* activity compared to that of the wildtype. Similarly, we found that expression of the *sdhC*::*lux* reporter increased steadily in the absence of a functional Cpx response, while the wildtype activity of the Cpx TCS lead to transcriptional repression of the *sdhC* promoter (**Figure 1C**).

To corroborate the luminescence profile of the control and ETC reporters in liquid LB medium, we also examined expression of the reporter genes on solid media (**Figure 1D**. The patterns of p*nuo*::*lux*, p*sdhC*::*lux* and p*cpxP*::*lux* reporter activity observed on solid medium

resembled those in the liquid medium assay. In the wildtype strain, the p*cpxP*::*lux* reporter was strongly activated, while light was not detectable in a *cpxA* mutant background. This pattern was reversed for the p*nuo*::*lux* and p*sdhC*::*lux* reporters, that demonstrated low activity in the presence of the intact Cpx TCS (**Figure 1D**).

Since these results suggested Cpx-mediated repression of the *sdhC* promoter, we examined the region upstream of *sdhC* to determine if any CpxR binding sites could be identified. We identified a putative CpxR binding site approximately 150 bp downstream of the predicted *sdhC* transcription start site (TSS) by using Virtual Footprint (http://prodoric.tu-bs.de/vfp/vfp_promoter.php)(209)(**Figure 1E**). Together, our observations suggest that the expression of the *sdhCDAB* operon could be directly repressed by phosphorylated CpxR.

SDH activity is affected by excessive activation or absence of the Cpx response. Our experimental results with the *sdhC*::*lux* reporter predict that the rate of succinate oxidation performed by SDH will be decreased in the presence of an active Cpx TCS relative to a mutant lacking the Cpx response. To test this hypothesis, we assayed the levels of SDH enzyme activity in the wildtype, as well as *cpxR*::kan and *cpxA24* mutants, reflecting a deactivated and constitutively activated Cpx response, respectively (123). We also included a strain bearing the NlpE overexpression vector pTrc-*nlpE* to induce the Cpx response exogenously (**Figure 2**). In this assay, the oxidation of succinate is accompanied by the transfer of electrons to an artificial electron acceptor (probe), which changes colour depending on the enzymatic activity of the sample. When in oxidized state, the probe is blue with maximal absorption at 600 nm, whereas when reduced it is colourless. Our results demonstrate that the activity of the SDH complex is decreased upon activation of the Cpx system in both the *cpxA24* mutant and the NlpE overexpression backgrounds, as expected based on the repressive effect of the Cpx response on *sdhC*::*lux* expression observed in **Figure 1C and D** (**Figure 2A**). Interestingly, the loss of the Cpx response did not result in higher SDH activity, as might be anticipated with the relieved

inhibition of *sdhCDAB* transcription. In contrast, mutation of *cpxR* lead to diminished succinate oxidation rates. Surprisingly, the decrease in SDH activity in this background was equal to or greater than that observed in the presence of the strongly Cpx-activating *cpxA24* allele (**Figure 2B**). This is analogous to a previously observed decrease in the rate of oxygen consumption in the Δ*cpxR* mutant, despite the fact that transcription of the operons encoding NDH-I and cytochrome *bo₃* are upregulated in this background (179). Together, these findings suggest that the Cpx TCS not only transcriptionally regulates the SDH protein complex, but also regulates factors responsible for maintaining its proper activity and biogenesis.

The cellular need for the Cpx response increases when respiratory complexes are more prevalent or active. *E. coli* is capable of growing on a number of different sugar substrates, generating the majority of its ATP via the process of oxidative phosphorylation (210). Carbon sources that cannot be utilized through the process of substrate-level phosphorylation, or fermentation, are called non-fermentable and require a functional ETC for sufficient energy generation. Such carbon sources include succinic acid (succinate), malic acid (malate) and glutamic acid (glutamate) (211–213). Poor growth of NDH-I mutants on either malate or succinate has been proposed to reflect low energy conservation efficiency due to a low level of ATP inside the cells (48). Previously reported data and our observations suggest that the Cpx TCS affects transcription and function of membrane complexes required for growth on non-fermentable carbon sources, including those associated with electron transport, the TCA cycle and oxidative phosphorylation (**Figure 1B-D**)(145, 179). This led us to hypothesize that the activity of the Cpx pathway would be necessary under conditions that create increased demand for respiration. We measured transcription of the operons encoding membrane bound respiratory complexes together with a Cpx-regulated gene by spotting strains bearing transcriptional luminescent reporter plasmids containing p*nuoA*::*lux,* p*sdhC*::*lux,* or p*cpxP*::*lux*

promoter fusions on minimal medium supplemented with a glucose-succinate carbon source gradient (**Figure 3**).

Expression of the p*cpxP*::*lux* reporter increases as the concentration of succinate increases, whereas in the presence of glucose p*cpxP*::*lux* demonstrates background levels of luminescence comparable to the empty vector control. Notably, none of the reporters were activated to high levels in the presence of glucose, which supports our hypothesis that growth under conditions that increase demand for respiratory complexes leads to Cpx pathway activation. Due to high p*cpxP*::*lux* activity, p*nuoA*::*lux* and p*sdhC*::*lux* promoter activities were not detected by the imaging system on short exposure times, therefore we spotted the strains containing ETC reporters on a different plate and assayed them separately to image the lower luminescence activity (**Figure 3**). It can be seen that the activity of the p*nuoA*::*lux* and p*sdhC*::*lux* reporters increases commensurately along the succinate concentration gradient. Notably, the expression of these reporters was much higher in the absence of the Cpx response, which supports our previous findings (**Figure 1A**).

To better understand how the Cpx response is activated by respiration, we wanted to see if increasing the concentration of glucose in the medium containing succinate would relieve the envelope stress and reduce Cpx activity. Indeed, the activity of the p*cpxP*::*lux* reporter gradually decreased when the glucose concentration increased in the medium (**Figure 3**). Based on the results of this experiment, we can conclude that the cellular need for Cpx-mediated stress adaptation increases when respiratory complexes are in increased demand.

The Cpx response regulates NuoA protein levels. The Cpx response was shown to directly repress the transcription of the *nuo* operon to ensure envelope integrity during stress and reduce excessive protein traffic within the IM (179)(**Figure 1B**). A previous report has shown that oxygen consumption was reduced in cells with either an activated or inhibited Cpx response, which led to the hypothesis that the Cpx TCS regulates respiratory complexes post-

transcriptionally (179). To determine whether the Cpx response regulates NuoA protein expression beyond transcription, a plasmid that expresses a triple FLAG-tagged NuoA subunit of the NDH-I complex from an exogenous, IPTG inducible promoter was constructed previously (214). Given that the NuoA-3×FLAG construct is expressed from a CpxR-independent promoter, any effects of Cpx pathway activity on NuoA protein levels should be independent of its transcription. NuoA protein specifically was chosen due to its structural role in the assembly of the NDH-I peripheral arm (192). It has previously been demonstrated that the NuoA-3×FLAG protein amount was reduced when the Cpx response was constitutively activated and slightly increased in the absence of Cpx response (214). To gain more insight into how the activity of the Cpx response affects protein turnover over time, we performed a protein stability assay by utilizing the total protein synthesis inhibitor chloramphenicol and monitored the rate of NuoA-3×FLAG degradation over 120 minutes after translation had been halted (**Figure 4**). Relative quantification of the bands showed that in the absence of the Cpx response, approximately half of the starting amount of NuoA-3×FLAG protein was degraded in 45 minutes, which was 25 minutes longer than in the wildtype strain, indicating slower protein turnover (**Table 3**). Unexpectedly, the rates of NuoA-3×FLAG degradation over the course of the experiment were comparable between the *cpxA24* and the wildtype strains, although the total amount of protein degraded by the end of the experiment was larger in the *cpxA24* (**Figure 4; Table 3**). Together, our results suggest that Cpx-regulated protein degrading factors are responsible for faster and more efficient turnover of NuoA-3×FLAG proteins in the WT strain, and that the decreased rate of degradation seems to be the reason for the larger amount of NuoA observed in Cpx-deactivated background.

Cpx-regulated protein folding and degrading factors affect growth during high respiratory demand. We found that the rate of NuoA-3×FLAG proteolysis was reduced when the Cpx response was abolished, suggesting that the wildtype activity of the Cpx pathway

assisted protein turnover (**Figure 4**). Given that bacteria with a compromised ETC are not able to generate sufficient amounts of ATP to support growth on non-fermentable carbon sources, we hypothesized that Cpx-regulated protein folding and degrading factors may impact the biogenesis of the ETC, together with the ability of the bacterial cells to generate proton motive force (PMF) and maintain their ATP levels. The candidate gene list for this experiment was derived from previous publications (145, 206) and unpublished RNASeq data. To identify genes of interest, a preliminary screening of several of these envelope-associated protein folding and degrading factors was performed previously (214). Several Cpx-activated genes were overexpressed in BW25113 Δ*nuoA* containing the NuoA-3×FLAG expression vector and NuoA-3×FLAG protein levels were analyzed by dot blot. Overexpression of the DegP, HtpX, PpiD, and YccA proteins had the largest impact on the abundance of NuoA-3×FLAG protein, resulting in a greater than 2-fold increase in the amount of NuoA-3×FLAG in comparison to the vector control (214). Furthermore, the activities of protease/chaperone DegP, the IM protease HtpX, YccA, a factor that modulates IM proteolytic activity, and PpiD periplasmic chaperone, have been previously implicated in maintaining the integrity of the envelope and responding to stress generated by protein misfolding (87, 110, 131, 145, 215).

To investigate the role these proteins may have in the quality control of the ETC complexes, we analyzed growth of the knockout mutants on minimal media supplemented with glucose, succinate or malate in BW25113 *E. coli* (**Figure 5**)(204). As shown in **Figure 5**, deleting *cpxR, ppiD, yccA, htpX* or *degP* resulted in growth defects of differing severity in comparison to the wildtype. All strains were able to grow on media supplemented with glucose, where their growth would not solely depend on energy generated via respiration. In addition, we noticed that the growth phenotypes of some mutants were distinct depending on whether the media contained malate or succinate as a carbon source. Our data demonstrate that the growth of Δ*cpxR*, Δ*ppiD* and Δ*yccA* mutants was severely attenuated when grown in media

supplemented with malate, whereas the defect was less pronounced in the succinate condition. Notably, deletion of genes encoding inner membrane protease HtpX and periplasmic protease/chaperone DegP resulted in more modest growth defects. This result was unexpected, as Cpx-mediated regulation of these proteolytic factors has previously been identified as important in envelope protein quality control (110, 216). Together, these data suggest that the absence of a functional Cpx system and several associated protein folding and degrading factors compromises proper biogenesis of the ETC, specifically the NDH-I complex, resulting in decreased viability in media that creates high respiratory demand.

Cpx-regulated protein folding and degrading factors affect NuoA protein levels. Our results implicate the Cpx-controlled protein quality control factors YccA and PpiD in the biogenesis of membrane-bound ETCs, and to a lesser extent the proteases DegP and HtpX (**Figure 5**). We therefore sought to examine the impact of Δ*ppiD*, Δ*yccA*, Δ*degP* and Δ*htpX* knockouts on NuoA-3×FLAG abundance via western blotting. We demonstrated that deletion of these Cpx-regulated protein folding and degrading factors altered NuoA-3×FLAG protein levels compared to the wildtype (**Figure 6**). Deletion of DegP, PpiD, YccA or HtpX increased NuoA-3×FLAG abundance by a factor of 5.56, 4.83, 3.95 and 1.49, respectively, in comparison to the wildtype. Although the specific fold changes in NuoA-3×FLAG levels varied between biological replicates of this experiment, we consistently detected an increased amount in the mutant strains relative to the wildtype (**Figure 6**). In agreement with the previous findings, where deletion of CpxR resulted in a mild accumulation of NuoA-3×FLAG (214) and a slower turnover rate (**Figure 4**), we observed accumulation of NuoA-3×FLAG in the Δ*cpxR* mutant (**Figure 6**).

Since the absence of envelope quality control factors generally led to increases in NuoA-3×FLAG protein levels, we next asked how the degradation of NuoA-3×FLAG was affected over time in these mutants. We performed a similar protein stability assay to the one

described above, where we monitored the levels of exogenously produced NuoA-3×FLAG over 120 minutes after the addition of total protein synthesis inhibitor chloramphenicol. Interestingly, we observed nearly complete NuoA-3×FLAG degradation only in the case of Δ*ppiD*, whereas in Δ*yccA*, Δ*degP* and Δ*htpX* mutants NuoA-3×FLAG protein was not degraded until the end of the experiment (**Figure 7**). The absence of DegP periplasmic chaperone/protease seemed to have the strongest effect on stabilization of NuoA-3×FLAG with 22% of the protein still present after 120 minutes (**Figure 7, Table 4**). It is important to note that this experiment was only performed once for the wildtype sample, and it needs to be repeated to gain more information about the trends. Taken together, our results demonstrate that Cpx-regulated protein folding and degrading factors affect abundance and turnover of the NuoA protein, and support the hypothesis that the Cpx response regulates the NDH-I complex at the post-translational level.

CpxQ sRNA affects the stability of the *sdhC* transcript. As activation of the Cpx response reduces expression and abundance of the ETC proteins, we wanted to know whether the non-coding arm of the Cpx response was involved in post-transcriptional regulation of the respiratory complexes. The identity of discovered CpxQ targets suggests that under envelope stress CpxQ acts cooperatively with the rest of the Cpx pathway to restore membrane homeostasis. Excessive production of CpxQ-regulated targets was shown to compromise the integrity of the IM and consequently induce the Cpx pathway (176). Interestingly, one of the first CpxQ-associated phenotypes described was the repression of the sodium-proton antiporter NhaB, which when overexpressed led to reduced membrane potential (176). Given that the majority of proton pumping activity in the cell is performed by the complexes of the ETC, we wondered if CpxQ affects their transcript levels. The possibility of such regulation is supported by the fact that during envelope stress or nutrient limitation, other sRNAs, including RyhB, RybB and Spf, are known to regulate the respiratory complexes, such as NDH-I and SDH (165,

217). To begin to investigate this possibility, we first used the IntraRNA RNA-RNA interaction prediction algorithm (218–221), which suggested that the CpxQ sRNA binds *sdhC* mRNA with both of its seed regions R1 and R2 (176), and that this interaction takes place within the coding sequence (CDS) of the *sdhC* gene (**Figure 8A**). Other sRNAs have been demonstrated to bind in similar regions within the CDS, and such mechanism of regulation downstream of the ribosome binding site (RBS) is relatively novel and was shown to both positively and negatively affect mRNA transcripts. For instance, binding of an sRNA within the CDS can both stimulate an RNaseE-dependent cleavage of the target mRNA (222) and prevent it by hiding a cleavage site from RNase E (223). Alternatively, sRNA binding deeper into the coding sequence can interfere with formation of inhibitory RNA structures that prevent translation (151, 222). To see if any of these mechanisms could potentially be employed by CpxQ, we analyzed the secondary structure of the *sdhC* mRNA using RNAfold software (224). The RNAfold algorithm was used to predict the most favourable minimum free energy structure and visualise where exactly the putative CpxQ binding site could be located (**Figure 8B**).

Previously performed microarray analysis indicated a dozen repressed transcripts in the presence of transiently induced CpxQ, most of which were found to encode membrane-associated proteins (176). Given that the ETC complexes are composed of multiple subunits, some of which are transmembrane and require proper insertion into the IM, and that their excessive activity has been shown to activate the Cpx response, we hypothesized that their transcripts could be regulated by CpxQ. To determine this, we grew MC4100 *E. coli* to OD$_{600}$ ~0.35, induced (10 min) the expression of CpxQ sRNA from a plasmid-borne arabinose-inducible promoter (P*ara*) and collected RNA. We assayed changes in mRNA levels using quantitative PCR (qPCR). We looked at the expression of the *nuoA* (NuoA subunit of NDH-I), *cyoA* (CyoA subunit of cytochrome *bo₃*) and *sdhC* (SdhC subunit of SDH) genes, as well as the *gyrA* (subunit A of DNA gyrase) gene, which was used as an endogenous control since it

41

is not known to be Cpx-regulated. We found that overexpression of CpxQ led to an ~17-fold increase in the level of *sdhC* transcript (**Figure 9**), whereas the expression of other genes was not significantly affected. This result was unexpected since i) CpxQ was previously shown to negatively affect the stability and translation of its targets and ii) Cpx response activation results in lower levels of transcription and activity of the SDH complex (**Figure 1C and D, Figure 2**).

To eliminate the possibility of *sdhC* mRNA levels being influenced by the addition of the alternative carbon source, we included the strain carrying an empty pBAD18 vector induced with arabinose (**Figure 9**). We consider this effect unlikely since we used MC4100 strain of *E. coli* that cannot utilize L-arabinose for growth due to a chromosomal mutation *araD139* (225). Normally, *araD* encodes for L-ribulose-5-phosphate 4-epimerase that is required for conversion of L-ribulose 5-phosphate to D-xylulose-5-phosphate, which in turn enters the pentose phosphate pathway to generate further metabolites and reducing equivalents. Inability to fully process arabinose leads to accumulation of L-ribulose 5-phosphate in the cell (225), hence should not lead to any metabolic changes that may impact succinate dehydrogenase. Indeed, addition of arabinose did not cause the levels of stabilization of the *sdhC* transcript observed in the CpxQ-overexpressing strain (**Figure 9**) and did not have a significant effect on the other assayed genes.

DISCUSSION

The Cpx response is believed to mediate adaptation to stresses that result in envelope perturbations through a variety of mechanisms, including facilitating degradation of misfolded or mislocalized proteins. Until recently, there was only a small number of proteins whose stability was known to be affected by the Cpx stress response, however the breadth of characterized Cpx-mediated adaptations continues to expand. It was recently demonstrated that the Cpx response regulates the expression of the genes encoding NDH-I and cytochrome *bo₃*,

large envelope complexes involved in aerobic respiration (179). Transcriptional repression of the *nuo* and *cyo* promoter regions under stress is thought to reduce production of new respiratory complexes and prevent excessive protein traffic within an already compromised cell envelope. Interestingly, when the rates of oxygen consumption were compared between $\Delta cpxRA$ and wildtype EPEC, it was found that despite increased transcription of the genes encoding NDH-I and cytochrome bo_3 in the $\Delta cpxRA$ EPEC mutant, the activity of the aerobic ETC was still impaired (179). These discoveries suggested a novel role for the Cpx TCS in monitoring protein biogenesis and regulating factors, potentially impacting the function, stability, and assembly of respiratory complexes beyond transcription.

In this study, we provide evidence that the Cpx response regulates succinate dehydrogenase, the only enzyme of the TCA cycle that interacts directly with the ETC chain, being central to cellular metabolism and energy conversion (184, 186, 198, 226, 227). Raivio *et al.* reported the *sdhCDAB* operon among genes whose transcription was downregulated upon transient NlpE overexpression along with other genes involved in respiration, including the *nuo* and *cyo* operons (145). In agreement with this finding, we show that the Cpx TCS inhibits the activity of p*sdhC*::*lux* reporter in a wildtype strain grown in the absence of exogenous stresses, whereas in the absence of a functional Cpx response, p*sdhC*::*lux* expression is elevated (**Figure 1C, D**).

How might this operon be regulated by the Cpx response? Previous studies have shown that many Cpx-regulated genes contain a CpxR binding site within 100 bp of their transcriptional start site (206). Given that both *nuo* and *cyo* promoter regions possess CpxR binding sites, and their transcription is thought to be altered though direct binding of CpxR, it is possible *sdhCDAB* is regulated similarly since we identified a putative CpxR binding site approximately 150 bp downstream of the *sdhCDAB* TSS by using Virtual Footprint software (179, 209). Binding of CpxR response regulator between the TSS and the translation start site

would block transcription elongation from the *sdhC* promoter, decreasing the overall rate of *sdhCDAB* transcription. It is important to note though that this site deviates from the "perfect" CpxR consensus binding sequence (5′-GTAAA(N_5)GTAAA-3′), possessing a 6 bp linker and containing a GTTAA sequence in the 5' half of the binding site (**Figure 1E**)(228). Interestingly, this putative CpxR binding site is located in the *sdhCDAB* promoter region together with those of several other transcriptional regulators; ArcA possesses four binding sites up- and downstream of the *sdhCDAB* operon (229, 230) and the cyclic adenosine monophosphate (cAMP)-cAMP receptor protein (CRP) complex, which binding site is located approximately 94 bp upstream of the *sdhC* TSS (231, 232). Other known regulators of *sdhCDAB* operon include Fur (233, 234), Fnr (230) and several sRNAs shown to inhibit *sdhCDAB* mRNA translation (158, 165, 235). It is possible that some of these regulators may work in combination with CpxR or other members of the Cpx TCS to regulate the transcription and/or translation of the *sdhCDAB* operon in response to environmental changes.

Our results indicate that the wildtype activity of the Cpx pathway leads to transcriptional repression of the *sdhCDAB* gene cluster. We hypothesized that the SDH enzymatic activity will also be affected by the Cpx pathway and examined the rates of succinate oxidation by SDH in different Cpx backgrounds (**Figure 2**). We found that both NlpE overexpression and constitutive activation of the Cpx response resulted in decreased SDH activity, which is consistent with a decrease in *sdhCDAB* expression under these conditions (**Figure 2**)(145). Unexpectedly, we observed similarly low succinate oxidation activity in a mutant lacking the Cpx pathway, which correlated with the observations reported by Guest *et al*. (179). They demonstrated that a Δ*cpxRA* mutant strain had reduced oxygen consumption relative to the wildtype strain, presumably mediated by the enzymatic activities of the NDH-I and cytochrome *bo₃* complexes. Evidently, both the excessive induction and the absence of the Cpx stress response leads to reduced performance of the SDH complex, directly affecting both

the transcription of the *sdhCDAB* operon, while also influencing the activity of the enzyme itself.

Given the role of the Cpx TCS in detecting and responding to potentially lethal misfolded proteins at the IM, it has been hypothesized that its housekeeping activity contributes to proper folding, stability and regulated turnover of large envelope complexes (58, 121, 145, 206). While a significant portion of the Cpx regulon consists of proteases and chaperones that address protein misfolding at the IM, there are no known Cpx-regulated proteolytic factors involved specifically in degradation or stability of the ETC. Nevertheless, general polypeptide misfolding can be recognized by other non-specific proteases, including HtpX, DegP and FtsH, which are known responders to envelope stress, and are either directly or indirectly regulated by the Cpx pathway (39, 104, 105, 108, 110, 216, 236). The absence of such quality control in a *cpxR* knockout mutant could lead to aberrant complex formation and unproductive interactions between subunits of the respiratory complexes, leading to loss of function.

Envelope stress can be exacerbated by the presence of respiratory complexes; however, in *E. coli* this stress is not likely to be due to disruption of the proton gradient, as the Cpx response was not induced by the chemical protonophore CCCP (179, 237). We found that the increased demand for respiratory complexes resulting from utilization of non-fermentable carbon sources acts as an inducing cue for the Cpx response (**Figure 3**)(238). Past studies demonstrated that bacteria carrying mutations in genes encoding components of the ETC and quinone biosynthesis exhibit growth defects on succinate, malate, lactate, and acetate (48, 212, 213, 239, 240). In the absence of the Cpx response, or Cpx-regulated protein folding and degrading factors, a similar growth phenotype is seen (**Figure 5**). It is possible that in order to generate sufficient energy from non-fermentable carbon sources, bacterial cells upregulate expression and/or activity of respiratory protein complexes, which can then be subject to

misassembly, irreparable damage or insertion into an already compromised membrane, a situation that would necessitate a functional Cpx envelope stress response.

Under conditions in which damaged and/or misfolded proteins are predicted to accumulate, upregulation of protein folding and degrading factors constitutes a part of Cpx-mediated adaptation (121, 241). Regulation of proteolysis at the inner membrane of *E.coli* is one of the least characterised parts of the Cpx response, and is essential for maintaining the integrity of envelope biogenesis (111, 121, 125, 242). It has previously been proposed that the NuoA subunit of the NDH-I complex is subject to regulation by the Cpx pathway beyond transcription, and that constitutive activation of the Cpx response decreases the abundance of NuoA-3×FLAG protein (214). However whether this regulation occurred via post-transcriptional or post-translational mechanisms has not been distinguished. It has been demonstrated that the Cpx system regulates factors that inhibit translation, such as the CpxQ sRNA (176), therefore could decrease the amount of successfully translated *nuoA*-3×FLAG mRNA. Even though CpxQ has been previously proposed to play a role in preserving the PMF at the IM since it downregulates the sodium-proton antiporter NhaB and counteracts the loss of membrane potential caused by carbonyl CCCP treatment (176), our results demonstrate that CpxQ overexpression had no effect on the *nuoA* transcript levels (**Figure 9**).

In this study, we found that the efficiency of NuoA-3×FLAG protein turnover is reduced in the absence of the functional Cpx response (**Figure 4**) and hypothesized that activation of the Cpx response may result in increased proteolysis of NuoA proteins. This model is supported by the fact that the expression of IM-localized proteolytic factors responsible for quality control at the IM, including DegP, HtpX and the modulator of FtsH proteolysis YccA, are under the control of the Cpx response (110, 128, 130, 145, 206). Furthermore, our data demonstrates that loss of these factors results in growth defects in media that requires a functional ETC for survival, which is in agreement with the previously

suggested role of the Cpx response in the biogenesis of respiratory proteins (**Figure 5**)(179). Notably, strains lacking CpxR exhibited the slowest growth with a lag-phase extended to 30-40 hours (**Figure 5**). These findings strengthen the link between the ETC and the Cpx TCS, where in addition to direct transcriptional repression of respiratory complexes, the Cpx pathway regulates their biogenesis and turnover, likely through the controlled expression of protein folding and degrading factors.

Considering the impact the Cpx response has on aerobic respiration, why does the availability of relatively similar non-fermentable carbon sources in the medium yield such different growth outcomes (**Figure 5**)? Aside from ETC biogenesis regulation, the other key factor in the minimal media experiments is the differential energetics and interactions of the non-fermentable carbon sources with bacterial central catabolism. Despite being fed directly into the TCA cycle, malate and succinate differentially contribute to ETC bioenergetics. Malate and its oxidation product NADH are stronger reducing agents, with an E'_0 of -0.166V and -0.320V respectively, compared to succinate and its oxidation product $FADH_2$ with an identical E'_0 of +0.031V (243). Namely, the oxidation of malate resulting in NADH production, and subsequent oxidation of NADH by NDH-I provides more energy for ATP production. If NDH-I is functionally deficient, NADH-derived electrons cannot be utilized directly for proton motive force generation, given that the NDH-II complex is not involved in proton translocation (244, 245) and ATP generation is dependent on the proton-pumping activity of the downstream cytochromes. This is supported by the fact that the inhibition of NADH oxidase subunit activity of NDH-I results in poor to no growth on malate (246). Therefore, removing factors potentially involved in the quality control of NDH-I may result in strong growth defects when malate is the sole carbon source, which is what we observed in the case of $\Delta yccA$, $\Delta ppiD$ and $\Delta cpxR$ mutants. It is possible that the ability to bypass NDH-I and metabolize succinate directly through succinate dehydrogenase results in better viability of these mutants.

We propose that several Cpx-regulated protein folding and degrading factors associated with the non-specific protease FtsH and SecYEG translocation affect biogenesis of NDH-I, and potentially other respiratory complexes. FtsH-mediated degradation of the SecY subunit of the SecYEG translocon prevents blocking of the translocase with inefficiently exported proteins and is modulated by the YccA integral membrane protein (99, 247). YccA itself can act as a competing substrate for FtsH, negatively affecting its proteolytic activity. While we did not determine whether the impact of YccA on the ETC complexes is direct or indirect, it appears to be implicated in their biogenesis given the impact of *yccA* deletion on growth requiring respiration (**Figure 5**) and stability of NuoA (**Figure 6 and 7**). One possibility is that under Cpx-inducing conditions, CpxR activates the expression of YccA, which in turn inhibits the FtsH protease and prevents excessive degradation of SecY subunit, allowing for damaged inner membrane proteins to be replaced. Alternatively, or in addition, YccA may directly interact with respiratory proteins stimulating their translocation during times of increased need. For example, van Stelten *et al.* have shown that wildtype YccA and its stabilized mutant *yccA11* stimulated secretion of a LamB-LacZ hybrid protein (247). We found that knocking out *yccA* led to growth defects on both malate and succinate minimal medium (**Figure 5**), significant accumulation (**Figure 6**), as well as slower turnover of NuoA-3×FLAG protein (**Figure 7**). One explanation for this result could be that a lack of YccA leads to excessive degradation of SecY by FtsH causing NuoA secretion and membrane insertion to become stalled, with consequent accumulation of NuoA-3×FLAG in the cytoplasm or a state inaccessible to proteases. Curiously, elevated levels of NuoA-3×FLAG protein were observed when YccA was overexpressed (214). One explanation for this apparently contradictory result could be that elevated YccA leads to FtsH saturation with its inhibitor, and a potential decrease in FtsH proteolytic function leading to accumulation of more NuoA-3×FLAG as a result of either an increased rate of secretion and/or a lack of proteolytic turnover.

Recent studies have shown that the periplasmic chaperone PpiD improves translocation efficiency by clearing the Sec translocon of newly translocated proteins (88), and localizes in close proximity to the lateral gate of the SecY channel (89). One of the proposed mechanisms of NDH-I translation suggests that the ribosome associated with *nuo* mRNA is directed to the Sec-translocon by the signal recognition particle, which tethers the mRNA to the IM and leads to further translation of the globular subunits (192). We hypothesize that the co-translational translocation and further assembly of NDH-I may be compromised in the absence of PpiD. This is supported by the fact that deletion of *ppiD* resulted in one of the strongest growth defects we observed (**Figure 5**). Alternatively, removing PpiD from the periplasmic chaperone network could have impacted translocation and assembly of other factors, potentially involved in NDH-I quality control. Similar to YccA, both deletion and overexpression of *ppiD* led to an increased amount of NuoA-3×FLAG protein in the cell (**Figure 6**)(214), however the entire amount of NuoA-3×FLAG was degraded by the end of the 2-hour stability assay (**Figure 7**). Interestingly, PpiD chaperone has also been associated with the FtsH interactome. Bittner and colleagues found that FtsH was responsible for degrading the PpiD-YfgM fusion complex (248). Thus, as with YccA, further experimentation will be required to ascertain the precise mechanism(s) by which PpiD impacts expression and function of ETC complexes, whether through secretion and/or direct or indirect proteolysis. Whether or not the PpiD periplasmic chaperone is a part of the Cpx regulon is a matter of debate (86, 242). Some evidence suggests that *ppiD* is either weakly or not at all regulated by the Cpx TCS, and is not specifically involved in envelope functions monitored by the Cpx pathway (87, 206). Nevertheless, our results suggest that PpiD plays an important role in envelope biogenesis, whose involvement in the assembly of the respiratory complexes, and regulation by the Cpx response, should be further explored.

When we measured the growth rates of Δ*degP* and Δ*htpX* mutants, we found that they affected growth on non-fermentable carbon sources differently from Δ*ppiD* or Δ*yccA*. We observed a relatively mild effect of *htpX* deletion on respiratory growth (**Figure 5**), causing less NuoA-3×FLAG protein to accumulate (**Figure 6**). HtpX functions as a protease with cellular roles complementary or overlapping those of FtsH (249), therefore its removal may not be as detrimental to the cell. In addition, deletion of *htpX* activates the Cpx response (110), which in turn regulates the biogenesis of the ETC complexes. Surprisingly, overexpression of HtpX was previously shown to lead to an almost 20-fold increase in the amount of NuoA-3×FLAG in comparison to the vector control (214). Earlier studies have demonstrated that HtpX can undergo rapid self-cleavage upon atypical conditions of partial cell lysis or extreme overproduction of HtpX, and that the self-cleaved product is inactive (104, 108). It is possible that artificial overexpression of HtpX could lead to its self-degradation or excessive proteolysis of other factors involved in the quality control of the respiratory complexes. Unlike other mutants possessing stronger growth defects in media supplemented with malate, Δ*degP* mutants grew slower in succinate minimal media (**Figure 5**) and demonstrated the strongest effect on the NuoA-3×FLAG stabilization in the cell (**Figure 7**) . Kihara and Ito demonstrated that DegP is involved in the degradation of the HflK subunit of the HflCK complex, which interacts with and regulates the ATP-dependent protease FtsH (115). Therefore, both overexpression and deletion of DegP could impact FtsH-mediated proteolysis indirectly through HflK. This hypothesis is supported by the fact that we see accumulation of NuoA-3×FLAG after both overproducing DegP and removing it (**Figure 6**)(214). However it is still unclear what role DegP plays in the quality control of the ETC components, it is possible that its role is indirect.

Cumulatively, our results suggest that activation of the Cpx response may stimulate FtsH proteolytic degradation and/or impact the secretion of the electron transport chain

proteins. In support of this hypothesis, overexpression of FtsH was previously shown to decrease NuoA-3×FLAG protein levels (214). However, since *ftsH* is essential in *E. coli* (106), we were unable to determine if it is required for Cpx-mediated degradation of NuoA-3×FLAG. A major future direction to expand on this study could involve deleting *ftsH* in a strain that carries the *sfhC21* allele, which suppresses the lethality of the *ftsH* null and assessing NuoA-3×FLAG levels (94).Alternatively, a strain in which *ftsH* is deleted and a second copy under control of an inducible promoter is present elsewhere in the chromosome can be utilized.

One of the major findings of this work is that another essential component of cellular energetics, the succinate dehydrogenase complex, is a member of the Cpx regulon and that its expression is downregulated in response to stresses sensed by the Cpx TCS. Furthermore, the housekeeping activity of the Cpx response is required for proper biogenesis and performance of succinate dehydrogenase, as evidenced by the fact that in the absence of the functional Cpx pathway SDH activity is impaired. Recent studies hypothesised that during normal biogenesis of the ETC complexes, some subunits may not assemble correctly, and these subunits engage in non-productive interactions that generate the stress sensed by the Cpx response (179). This hypothesis is further supported by our findings, where increased demand for respiratory complexes induces the Cpx pathway, possibly due to higher risk of protein misfolding. Subsequently, activation of the Cpx response results in upregulation of proteases that degrade existing complexes, possibly facilitate secretion and membrane insertion, and directly represses transcription of *nuo*, *sdhCDAB* and *cyo* operons. Intriguingly, we found that overexpression of the CpxQ sRNA increases the stability of *sdhC* mRNA through a mechanism that requires further investigation (**Figure 9**). One way CpxQ sRNA could increase the stability of *sdhC* transcript is to protect it from RNAseE-mediated decay. A typical RNAseE cleavage site is AU-rich (250) and has a consensus sequence (A/G)N↓AU, where ↓ represents the site of cleavage and N stands for any ribonucleotide (251). In the case of *sdhC* mRNA, the region

bound by CpxQ does not seem to contain an RNAseE cleavage site and is overall GC-rich (**Figure 8B**). The other explanation for our results could be the indirect effects CpxQ might have on *sdhC* mRNA levels. It is possible that CpxQ negatively regulates DNA-binding proteins involved in repression of *sdhCDAB* operon at the transcriptional level, or downregulates the expression of other regulatory factors that normally promote *sdhC* mRNA turnover.

To better understand the mechanism of *sdhC* stabilization in the cell, several other experiment have to be performed, including the validation of the CpxQ-carrying vector. It requires assaying levels of CpxP protein, known to be negatively regulated by CpxQ sRNA via western blotting. It is important to note that in wildtype cells, chromosomal levels of CpxP are low and undetectable by immunoblotting, therefore this experiment requires CpxP to be expressed from an exogenous promoter on a high-copy number vector compatible with pBR322_origin (130, 177). Additionally, the effect of CpxQ overexpression can be examined by assessing the decrease in the activity of NhaB Na^+/H^+ antiporter. Located in the inner membrane, NhaB is involved in regulation of intracellular pH at alkaline environments and maintaining low concentrations of intracellular Na^+ (252–254). Given that strains lacking major antiporters, including NhaB, NhaA and ChaA, cannot effectively export sodium, they are unable to grow in the presence of certain concentrations of NaCl (255). Possibly, overexpression of CpxQ sRNA and its inhibitory effect on NhaB can cause mild growth defects on media supplemented with higher sodium concentrations. Future experiments should be directed at assessing levels of SdhC-6×His protein in the cells where CpxQ was deleted or overexpressed. This will allow to distinguish between post-transcriptional and translational effects CpxQ might be having on the SDH complex.

Altogether, our results support a model in which the Cpx pathway maintains the function of critical cytoplasmic membrane protein complexes through modulation of an

intricate balance between transcriptional repression and increased protein turnover during periods of stress, while allowing for recovery of vital cellular activities including translocation of newly synthesized proteins and their insertion into the membrane as envelope stress is alleviated (**Figure 10**).

FIGURES AND TABLES

Table 1. Bacterial strains and plasmids used in this study

Strain or plasmid	Description	Source or reference
Bacterial strains		
MC4100	F$^-$, *[araD139]$_{B/r}$, Δ(argF-lac)169, λ$^-$, e14-, flhD5301, Δ(fruK-yeiR)725(fruA25), relA1, rpsL150(*StrR*), rbsR22, Δ(fimB-fimE)632(::IS1), deoC1*	(256)
VT2	MC4100 *cpxR*::kan	This study
E2348/69	Prototypical EPEC O127:H6 laboratory strain	(257)
RG222	E2348/69 *ΔcpxRA*	(179)
ALN195	E2348/69 *cpxA24*	(207)
BW25113	F$^-$, *Δ(araD-araB)567, lacI$^+$, ΔlacZ4787(*::rrnB-3*), λ$^-$, rph-1, Δ(rhaD-rhaB)568, hsdR514*	(202, 258)
TR10	MC4100 *cpxA24*	(123)
JW1818	BW25113 *htpX*::kan	(202)
JW0953	BW25113 *yccA*::kan	(202)
JW0431	BW25113 *ppiD*::kan	(202)
JW0157	BW25113 *degP*::kan	(202)
JW3883	BW25113 *cpxR*::kan	(202)
JW2283	BW25113 *nuoA*::kan; Kan^R	(202)
RG349	E2348/69 (pMPM-*nuoA*-3×FLAG)	This study
RG351	E2348/69 *cpxA24* (pMPM-*nuoA*-3×FLAG)	This study
RG350	E2348/69 *cpxR*::spc (pMPM-*nuoA*-3×FLAG)	This study
VT115	MC4100 (p*cpxP*-lux)	This study
VT123	MC4100 (pJW15)	This study
VT124	MC4100 (p*sdhC*-lux)	This study
RG57	MC4100 (p*nuoA*-lux)	(179)
VT130	MC4100 *cpxA*::cam (p*cpxP*-lux)	This study
VT131	MC4100 *cpxA*::cam (p*sdhC*-lux)	This study
VT132	MC4100 *cpxA*::cam (pJW15)	This study
VT133	MC4100 *cpxA*::cam (p*nuoA*-lux)	This study

TC220	MC4100 (pTrc-*nlpE*)	This study
RG480	BW25113 Δ*nuoA* derivative of JW2283	(179)
VT82	MC4100 (pBAD-CpxQ); Amp[100]	This study
VT95	MC4100 (pBAD18); Amp[100]	This study
VT175	BW25113 (pMPM-*sdhC*-6×His)	This study
Plasmids		
pFLP2	Broad host-range plasmid expressing the FLP recombinase from a temperature sensitive promote; Amp[R]	(259)
pJW15	Luminescence reporter vector plasmid	(205)
pJW15-p*cpxP* (pJW25)	Luminescence reporter plasmid containing *cpxP* promoter; Kan[R]	(207)
pJW15-p*nuoA*	Luminescence reporter plasmid containing *nuoA* promoter; Kan[R]	(179)
pJW15-p*sdhC*	Luminescence reporter plasmid containing *sdhC* promoter; Kan[R]	(179)
pMPM-K3	Low copy-number IPTG inducible cloning vector derived from pACYC184 and pBluescript; Kan[R]	(260)
pMPM-NuoA-3×FLAG	pMPM-K3 derived IPTG inducible *nuoA*-3×FLAG expression vector; Kan[R]	(214)
pTrc-*nlpE*	High copy-number expression vector with IPTG inducible *nlpE* promoter derived from pTrc99A vector; Amp[R]	This study
pMPM-SdhC-6×His	pMPM-K3 derived IPTG inducible *sdhC*-6×His expression vector; Kan[R]	

Table 2. Oligonucleotide primers used in this study

Primer name	Sequence
nuoAFLAGFwd	5'-TTTTAAGCTTCTTTTGATGAGTA-3'
nuoAFLAGRev	5'-TTTTTCTAGATTATTTATCATCATCATCTTTATAATCAATATCATGATCTTTATAATCGCCATCATGATCTTTATAATCGCGTTGACGATTAG CGATAC-3'
K1	5'-CAGTCATAGCCGAATAGCCT-3'
PsdhCFwdCln	5'-TTTTGAATTCGGTCTACCACTAATAACTG-3'
PsdhCRevCln	5'-TTTTGGATCCATGGAGAATGGACGCTATC-3'
nlpE_NcoI_F	5'-CGCACCATGGTGAAAAAGCGATAGTGACAG-3'
nlpE_WT_His_HindIII_R	5'-TGCCAAGCTTTTAGTGGTGGTGGTGGTGGTGCTCGAGCTGCCCCAAACTACTGCAATC-3'
pTrc99A_F	5'-GTTCTGGCAAATATTCTGAAA-3'
pTrc99A_R	5'-ATTTAATCTGTATCAGGCTGA-3'
P1cpxRFwd	5'-AACTATGCGCATCATTTGCTCC-3'
P1cpxR Rev	5'-CACATTAAATCGTTGGGCGGAT-3'
pBAD_fwd_primer	5'-ATGCCATAGCATTTTTATCC-3'
pBAD_rev_primer	5'-GATTTAATCTGTATCAGG-3'
CpxQ synthesis	5'-TAAGCAGAATTCTTTTCCTTGCCATAGACACCATCCCTGTCTTCCCCCACATGCTGTGGGGGTTTTTTTTCTAGATGCTTA-3'
NuoAFwdCpxQ	5'-CGCTCATCACTGGGCATTC-3'
NuoARevCpxQ	5'-CAACCGCCTACCAGCATCA-3'
CyoAFwdCpxQ	5'-GCATTGCTACCGTGAATGAAATC-3'
CyoARevCpxQ	5'-GGAGTTCATCACGGAGTTGGA-3'
SdhCFwdCpxQ	5'-CATCCGGTTCCCCATCAC-3'
SdhCRevCpxQ	5'-TGCCCACTGCAACAAAGGT-3'
GyrAFwdCpxQ	5'-CACCGCAACGCAAAACG-3'

GyrARevCpxQ	5'-TGATGGAGATAACCCCTTTCGT-3'
sdhC_FW_pMPM	5'- TCAG<u>GAATTC</u>CCGTAGTCCCCAGGGAATA-3'
sdhC_RV_pMPM	5'- AGC<u>TCTAGA</u>TTAGTGGTGATGGTGATGATGCCATACGAGGACTCCTGCGAGA-3'
M13F	5'-GTTTTCCCAGTCACGAC-3'
M13R	5'- CAGGAAACAGCTATGAC-3'

*Underlined sequences indicate restriction endonuclease cut sites (EcoRI: GAATTC, HindIII: AAGCTT, XbaI: TCTAGA)

**P1 transduction strains were verified by PCR using gene-specific forward primers (P1*genename*Fwd) and K1 reverse primer that binds inside of the kanamycin resistance gene.

Table 3. Relative band quantification calculated using Fiji (ImageJ) software for Figure 4.

Time, min	BW25113 WT	BW25113 ΔcpxR	BW25113 cpxA24
0	1	1	1
1	0.8736227	0.83863009	0.96293758
5	0.71124593	0.75016512	0.72735328
10	0.63119508	0.70426201	0.76737539
20	**0.49823794**	0.64889856	**0.44952824**
30	0.44765134	0.64664517	0.4140362
45	0.35571218	**0.47736897**	0.24964914
90	0.17522416	0.47630056	0.12982889
120	0.15862961	0.52593341	0.11517807

*Values represent relative quantification of the raw integrated density of the protein bands.

**The closest value representative of the protein half-life is highlighted in bold.

Table 4. Relative band quantification calculated using Fiji (ImageJ) software for Figure 7.

Time, min	BW25113 WT	BW25113 ΔyccA	BW25113 ΔppiD	BW25113 ΔdegP	BW25113 ΔhtpX
0	1	1	1	1	1
1	0.83374405	0.93688293	0.92098058	1.17040182	0.98632705
5	**0.48192521**	0.85176136	1.26342534	0.82381517	0.97774228
10	0.43805059	0.69154062	0.89942415	0.8361925	0.71405932
20	0.42149411	**0.43980649**	0.75259634	**0.56177711**	**0.47764135**
30	0.39400127	0.32036319	**0.50968982**	0.41197194	0.30520641
45	0.15763557	0.20774653	0.29886143	0.32736466	0.23410971
90	0.12271766	0.1318082	0.12956625	0.22191997	0.22272972
120	0.08679674	0.12842055	0.07468993	0.2274992	0.16344538

*Values represent relative quantification of the raw integrated density of the protein bands.

**The closest value representative of the protein half-life is highlighted in bold.

FIGURES

A

B
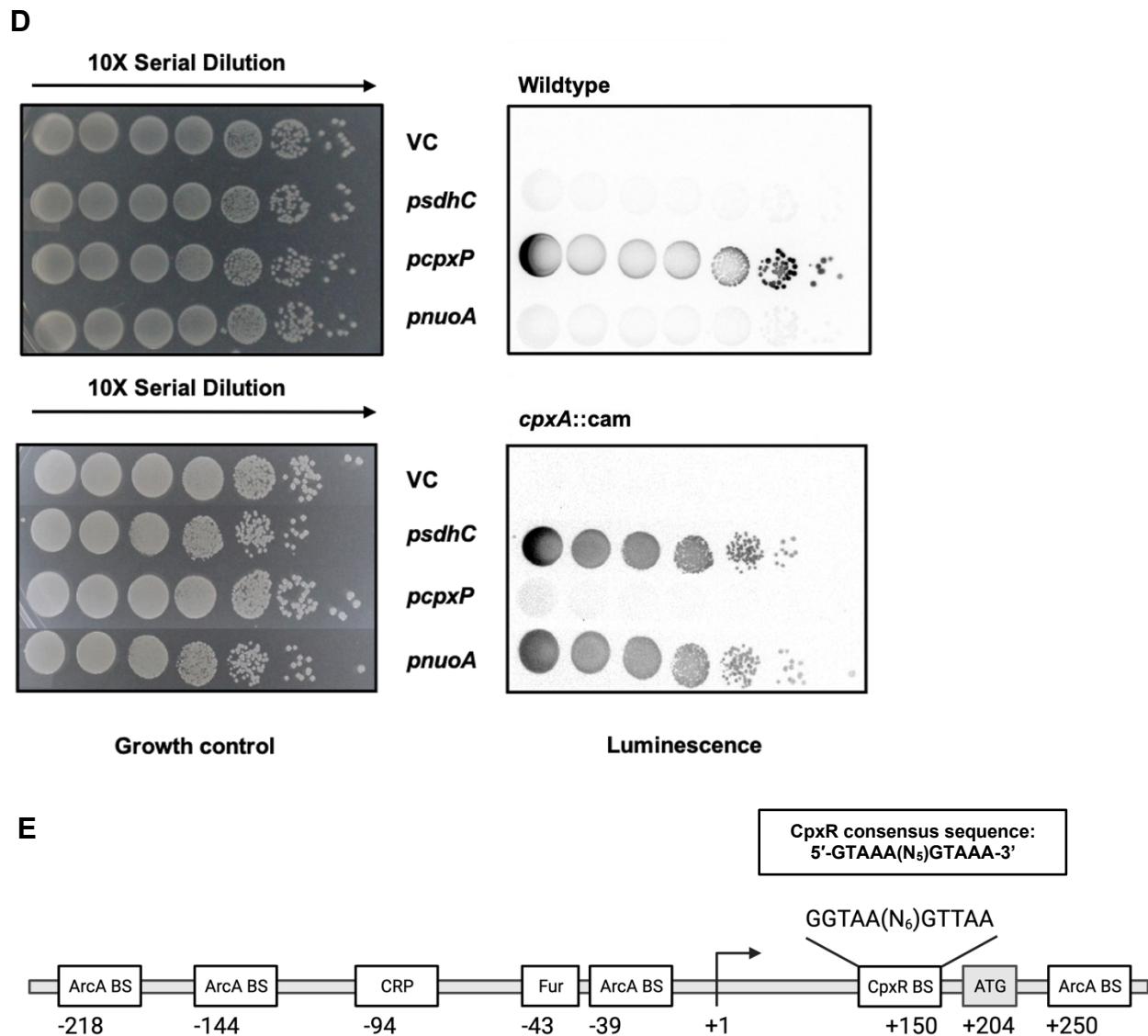

C

D

E
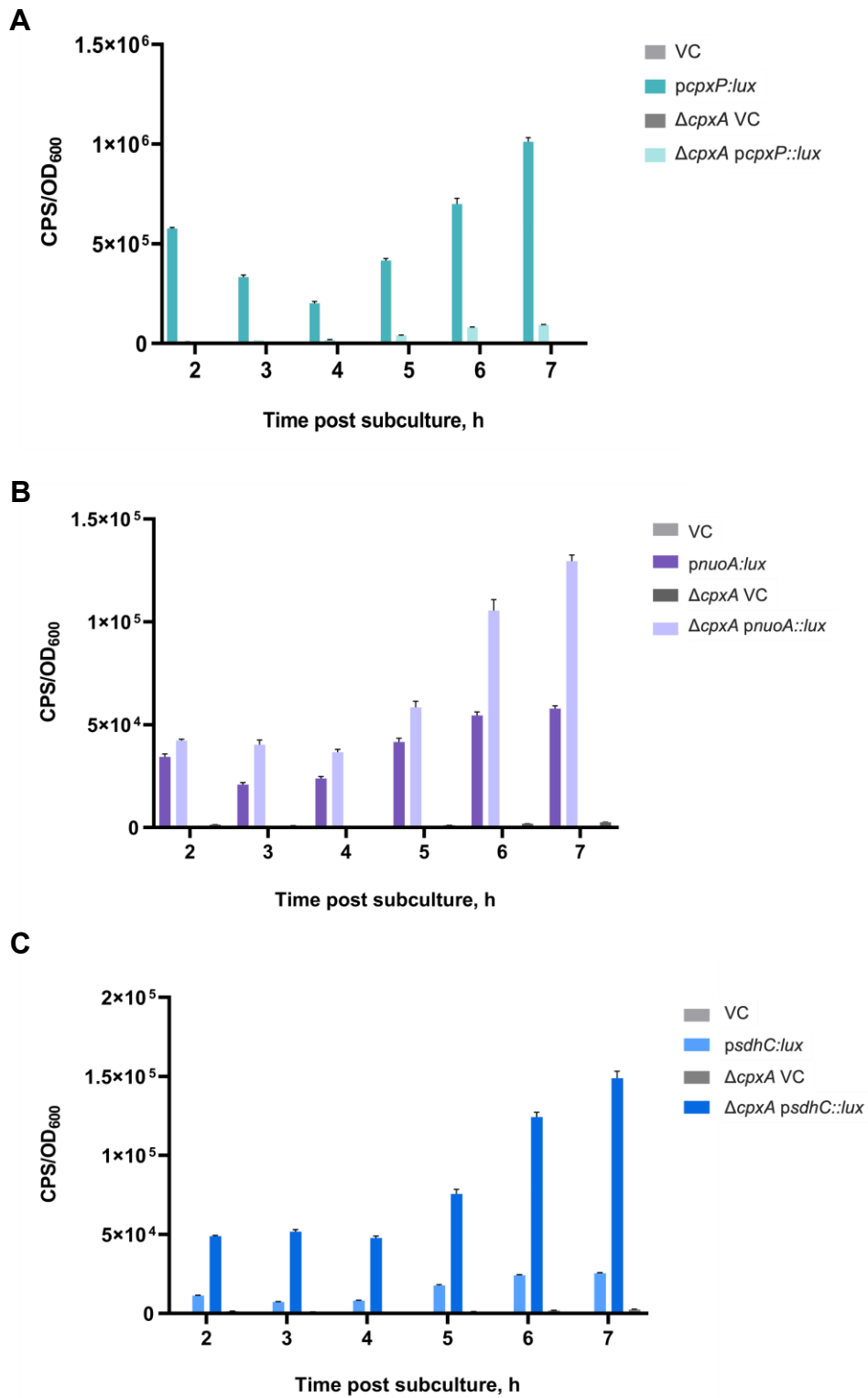
Figure 1. Transcription of the *sdh* operon encoding the succinate dehydrogenase complex is regulated by the Cpx stress response. Overnight cultures of wildtype *E.coli* MC4100 or a *cpxA*::cam mutant harbouring either pJW15 (vector control) or the **(A)** p*cpxP*::*lux,* **(B)** p*nuoA*::*lux*, or **(C)** p*sdhC*::*lux* reporter plasmids were subcultured 1:100 into fresh LB medium and incubated at 37°C with shaking. The luminescence and the OD_{600} were measured every hour for the duration of 7 hr and a final measurement was taken at 24 hr. Data correspond to the mean values from three biological replicates. Error bars depict standard deviations (SDs). **(D)** Luminescence activities are shown for wildtype *E. coli* MC4100 or a *cpxA*::cam mutant harbouring either pJW15 (vector control) or the p*nuoA*::*lux*, p*sdhC*::*lux* or p*cpxP*::*lux* reporter

plasmids. Luminescence was determined by imaging the luminescence of the strains grown on LB media plates for 24 hrs. **(E)** Schematic representation of the *sdhC* promoter region of BW25113 *E. coli* indicating the locations of the putative CpxR, ArcA, Fur and CRP-cAMP binding sites. Numbers indicate distances of the most upstream bp in each site from the transcription start site (+1) in base pairs. +, upstream; -, downstream; BS, binding site.
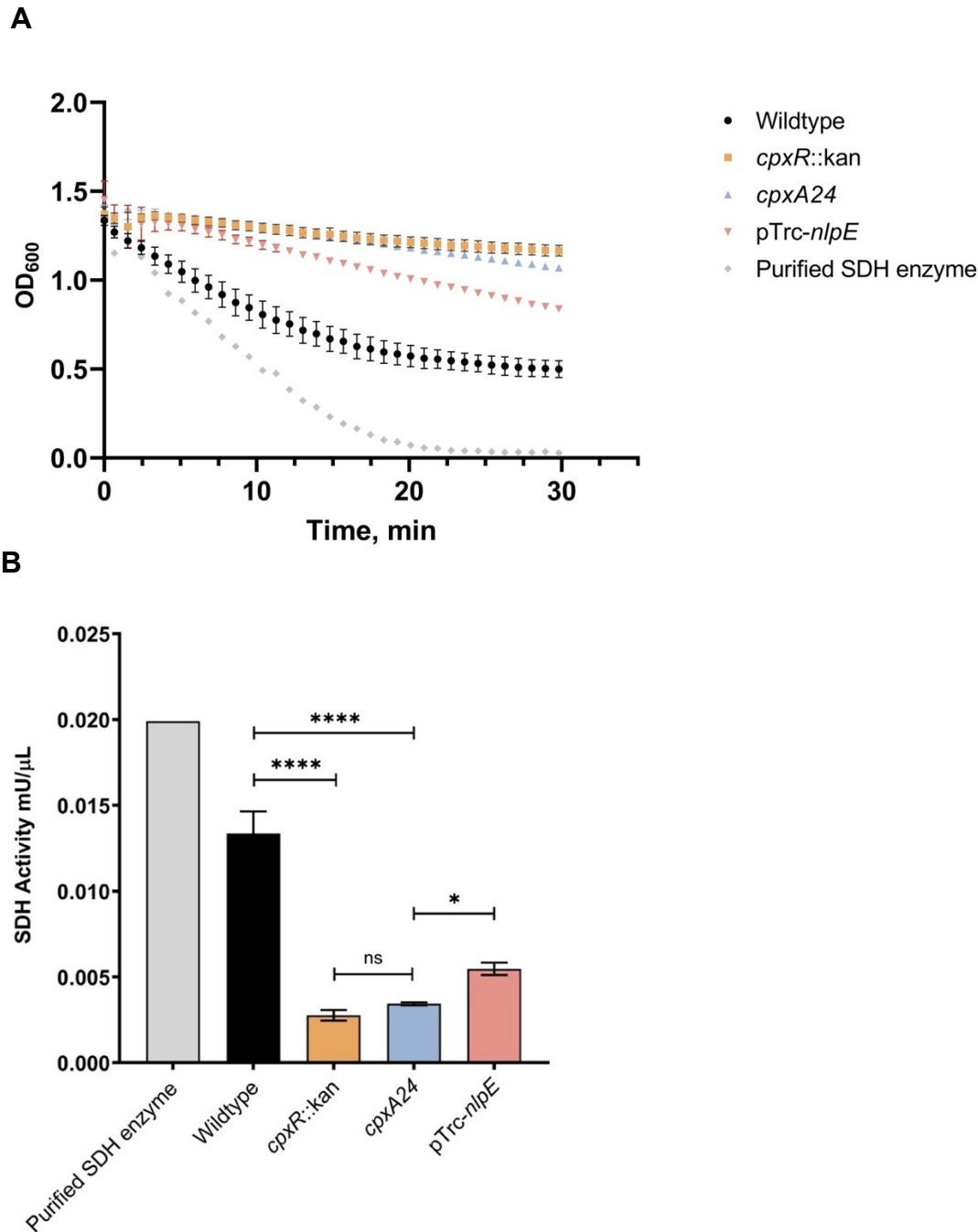
A

B

Figure 2. SDH activity is reduced by excessive activation or absence of the functional Cpx response. Wildtype MC4100, *cpxR*::kan, *cpxA24* and MC4100 harbouring NlpE overexpression plasmid (pTrc-*nlpE*) were subcultured from their overnight cultures 1:50 into 5mL fresh LB and grown to OD_{600} ~0.5 at 37°C with shaking. 1mL samples, standardized to the same optical density OD_{600}, were pelleted, and cell pellets were resuspended in 200µL of ice-cold SDH Assay Buffer (Abcam). Samples were prepared as per manufacturers' protocol,

loaded into a 96-well plate, and mixed with 50µL of SDH reaction mix (Abcam). **(A)** Assay data showing reduction of the DCIP artificial electron acceptor, accompanied by the colour change of the dye from blue to colourless (A_{600}). Absorbance at 600nm was measured every minute for 30 minutes at 25°C with shaking using the Cytation5^{TM} Cell Imaging Multi-Mode Reader (BioTek). **(B)** Succinate dehydrogenase activity of each sample was calculated as per manufacturers' protocol and plotted. All data correspond to the means and standard deviations of three replicate cultures. Asterisks indicate a statistically significant difference from the relevant wildtype control (****, $P \leq 0.0001$ [one-way ANOVA with Tukey's *post hoc* test]). NS indicates no statistically significant difference in SDH activity.
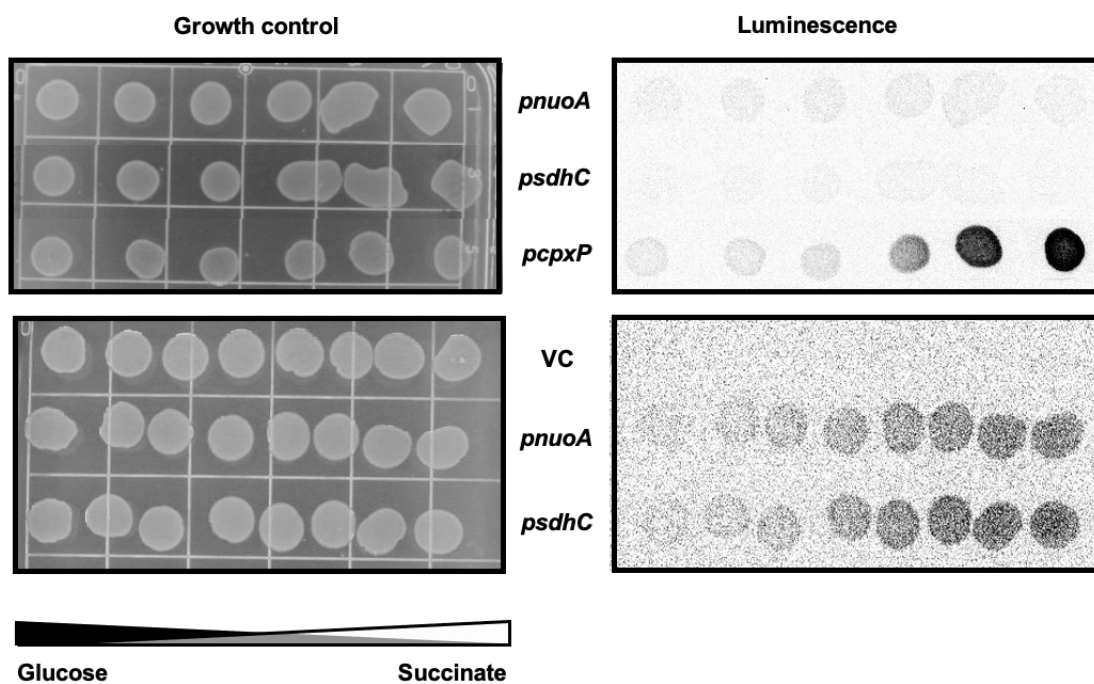
Figure 3. Demand for aerobic respiration due to the presence of non-fermentable carbon sources induces the Cpx pathway. Luminescence activities are shown for wildtype *E.coli* MC4100 harbouring either pJW15 (vector control) or the p*nuoA*::*lux*, p*sdhC*::*lux* or p*cpxP*::*lux* reporter plasmids. Luminescence of the strains growing on M9 minimal media plates containing a gradient of 0.4% glucose and 0.4% succinate, pH 7.0 was determined by imaging the luminescence of the spots after 48 hours of incubation at 37°C.
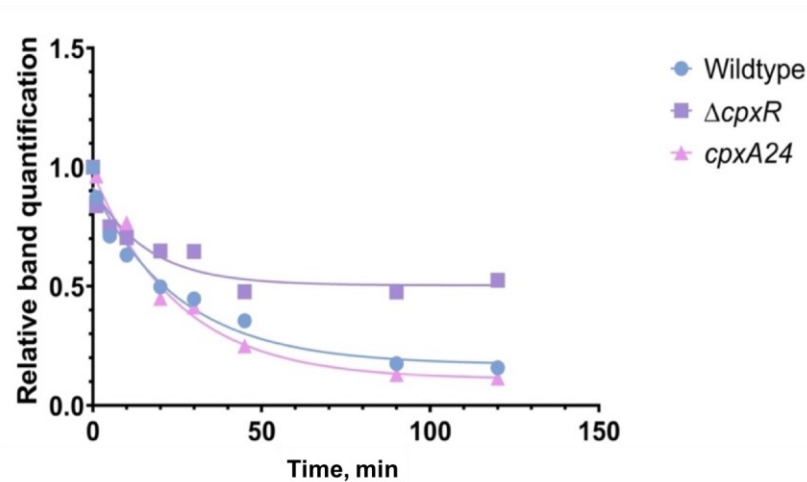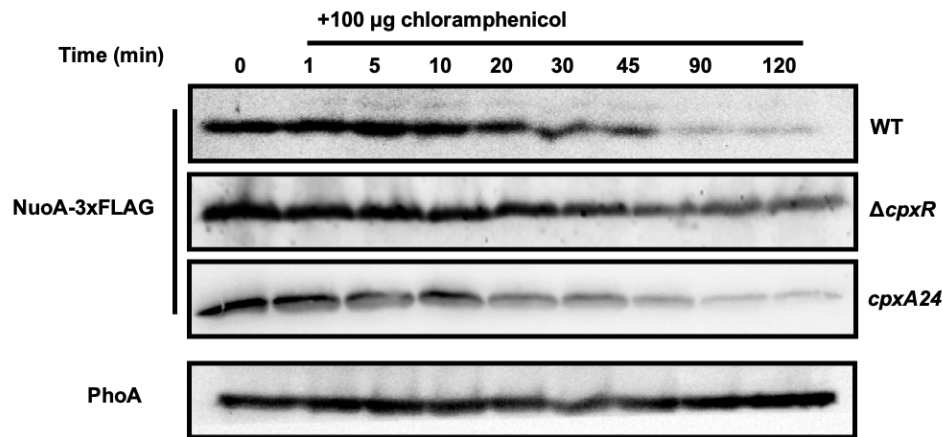
Figure 4. The Cpx response affects NuoA-3×FLAG protein levels. Wildtype BW25113 and the Δ*cpxR* or *cpxA24* mutants containing the pMPM-*nuoA*-3×FLAG expression vector were grown in 25mL LB at 37°C with shaking to an OD_{600} of 0.5. 0.1mM IPTG was then added to induce *nuoA*-3×FLAG expression, and bacteria were grown until an OD_{600} of 1.0 was reached. 100μg of chloramphenicol was added to inhibit protein synthesis, and 1mL samples were taken at 0 (before addition) 1, 5, 10, 20, 30, 45, 90 and 120 min after addition. Samples were loaded onto a 10% SDS polyacrylamide gel. NuoA-3×FLAG and alkaline phosphatase (PhoA) protein levels were determined via western blotting. PhoA protein levels served as a loading control. Proteins were detected using the Immun-Star alkaline phosphatase chemiluminescence kit (Bio-Rad) and the Bio-Rad ChemiDoc MP imaging system. Relative band quantification was performed using band intensity analysis in ImageJ. The protein stability assay data were fit

with a one-phase exponential decay curve to determine protein half-life using the Prism v7.0c
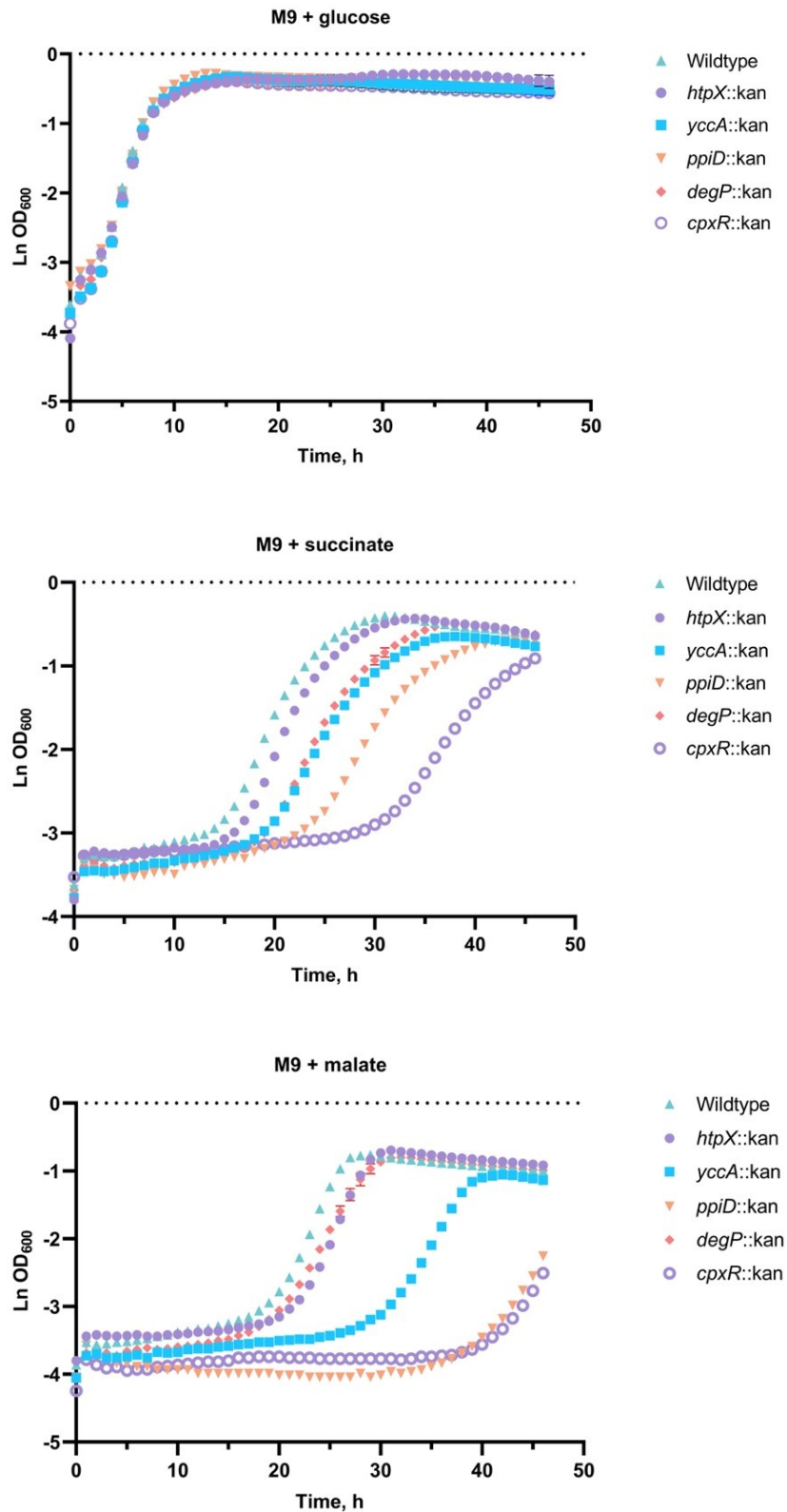
(GraphPad) software.

Figure 5. Deletion of several Cpx-regulated protein-folding and degrading factors results in growth defects in minimal media. Wildtype BW25113 and the mutants carrying the indicated gene deletions were grown overnight in LB at 37°C, washed twice in 1x phosphate-

buffered saline (PBS), and standardized to an OD_{600} of 1.0 in phosphate buffered saline. 10μL of the culture was subcultured into M9 minimal medium containing 0.4% glucose, 0.4% malic acid, pH 7.0 (malate) or 0.4% succinic acid, pH 7.0 (succinate), and grown for 48 hr at 37°C with 330 rpm linear shaking. Data correspond to the mean values from three biological replicates and are representative of three independent experiments. Error bars depict standard deviations (SDs).
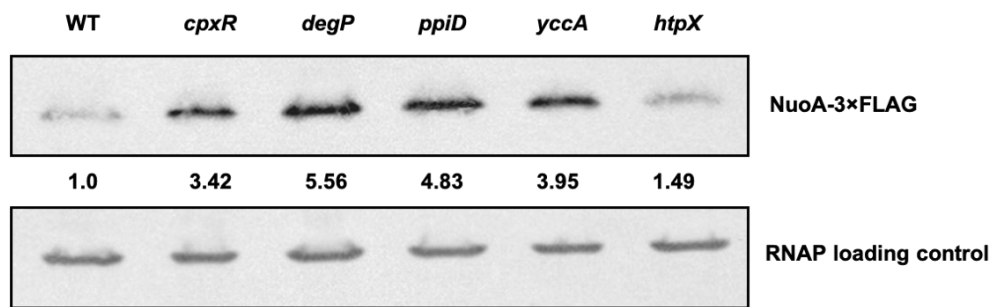
Figure 6. NuoA-3×FLAG protein levels are altered by deletion of several Cpx-regulated protein folding and degrading factors. Wildtype BW25113 and the mutants with the indicated gene deletions containing the pMPM-*nuoA*-3×FLAG expression vector were subcultured in 25mL fresh LB and grown at 37°C to an OD_{600} of 0.35. 0.1mM IPTG was added to induce *nuoA*-3×FLAG transcription and bacteria were grown for an additional 30 minutes. Samples were loaded onto a 12% SDS polyacrylamide gel. NuoA-3×FLAG and RNA Polymerase (RNAP) protein levels were determined via western blotting. RNAP protein levels served as a loading control. Membranes were imaged using the Bio-Rad ChemiDoc MP imaging system. Relative band quantification was performed using band intensity analysis in ImageJ.
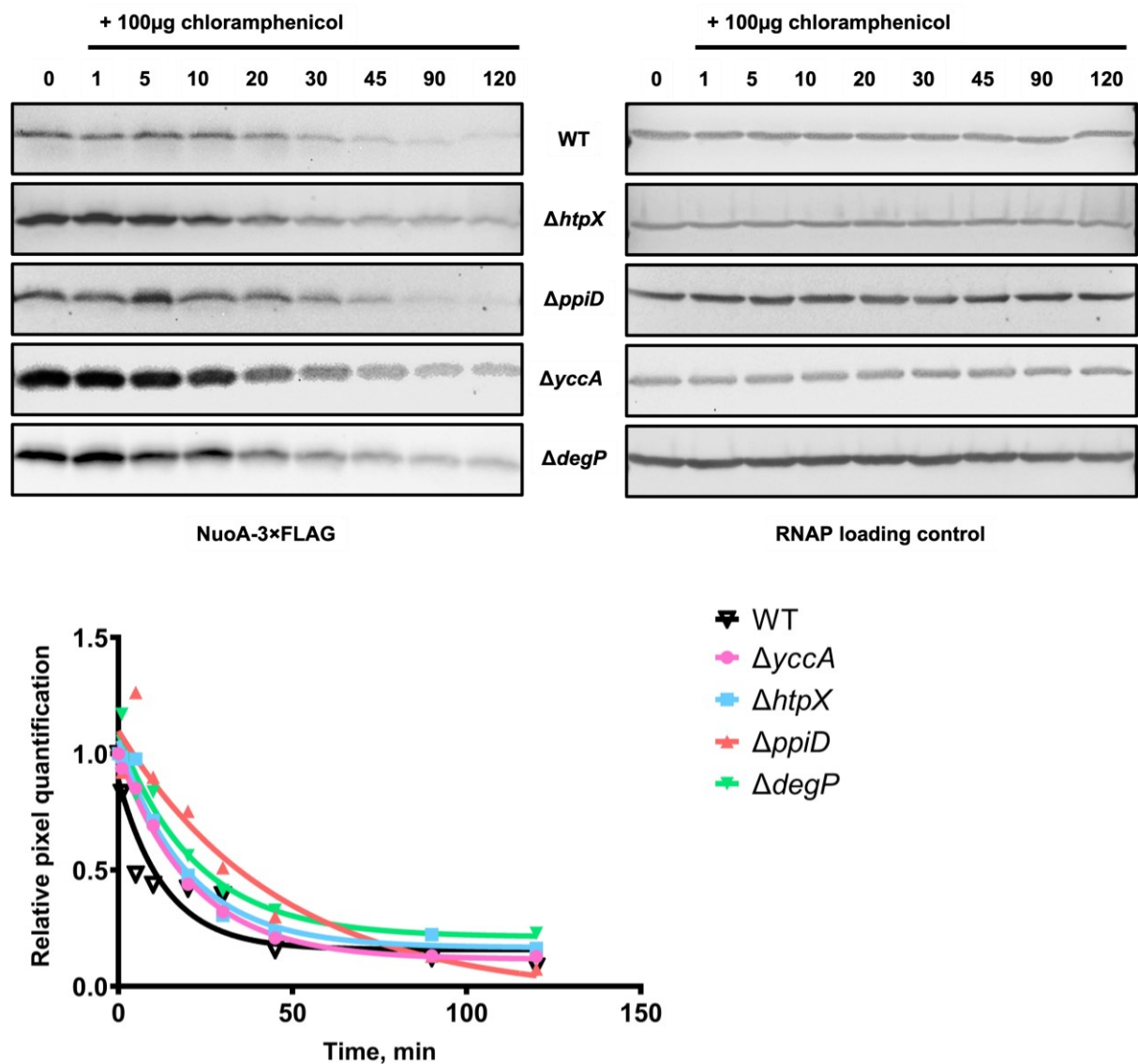
Figure 7. Turnover of NuoA-3×FLAG proteins is affected by deletion of several Cpx-regulated protein folding and degrading factors. Wildtype BW25113 *E. coli* and strains with indicated gene deletions containing the pMPM-*nuoA*-3×FLAG expression vector were subcultured in 25mL LB at 37°C with shaking to an OD_{600} of 0.5. 0.1mM IPTG was then added to induce *nuoA*-3×FLAG expression for 30 minutes. 100µg of chloramphenicol was added to inhibit protein synthesis, and 1mL samples were taken at 0 (before addition) 1, 5, 10, 20, 30, 45, 90 and 120 min after addition. Samples were loaded onto a 15% SDS polyacrylamide gel. NuoA-3×FLAG and RNA polymerase protein levels were determined via western blotting. RNAP protein levels served as a loading control. Protein bands were detected using the Bio-

Rad ChemiDoc MP imaging system. The experiment was performed in biological triplicate for the strains lacking protein folding and degrading factors, whereas the wildtype stability assay was only performed once and needs to be replicated. Relative band quantification was performed using band intensity analysis in ImageJ. The protein stability assay data were fit with a one-phase exponential decay curve to determine protein half-life using the Prism v7.0c (GraphPad) software.
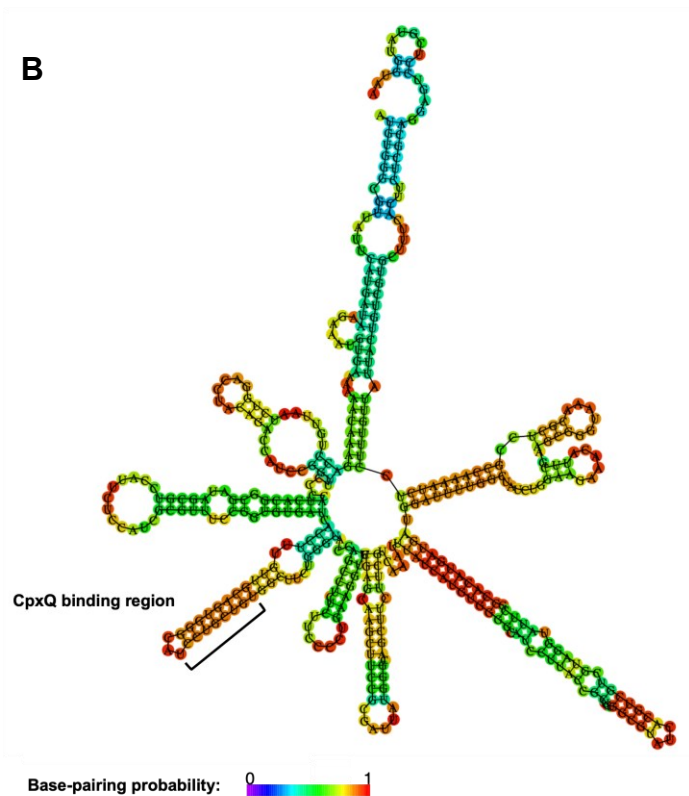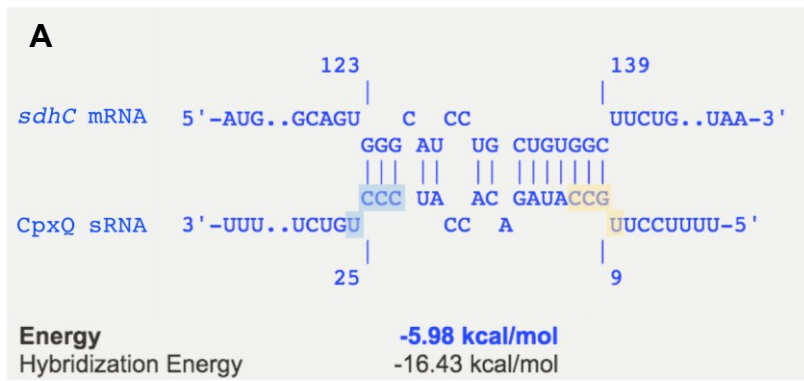
Figure 8. Model of interaction between the CpxQ sRNA and *sdhC* mRNA. (A) The CpxQ sRNA is predicted to bind within the open reading frame of the *sdhC* mRNA. The interaction between CpxQ sRNA and sdhC mRNA was predicted using IntraRNA software (218–221). Putative R1 and R2 seed regions of CpxQ are labeled yellow and blue, respectively. (B) Predicted minimum free energy secondary structure of *sdhC* mRNA. The structure is coloured by base-pairing probability, where 0 is low and 1 is high probability. The putative CpxQ binding site is indicated. Prediction of minimum free energy structure was performed using RNAfold Web Server provided by The ViennaRNA Web Services (224).
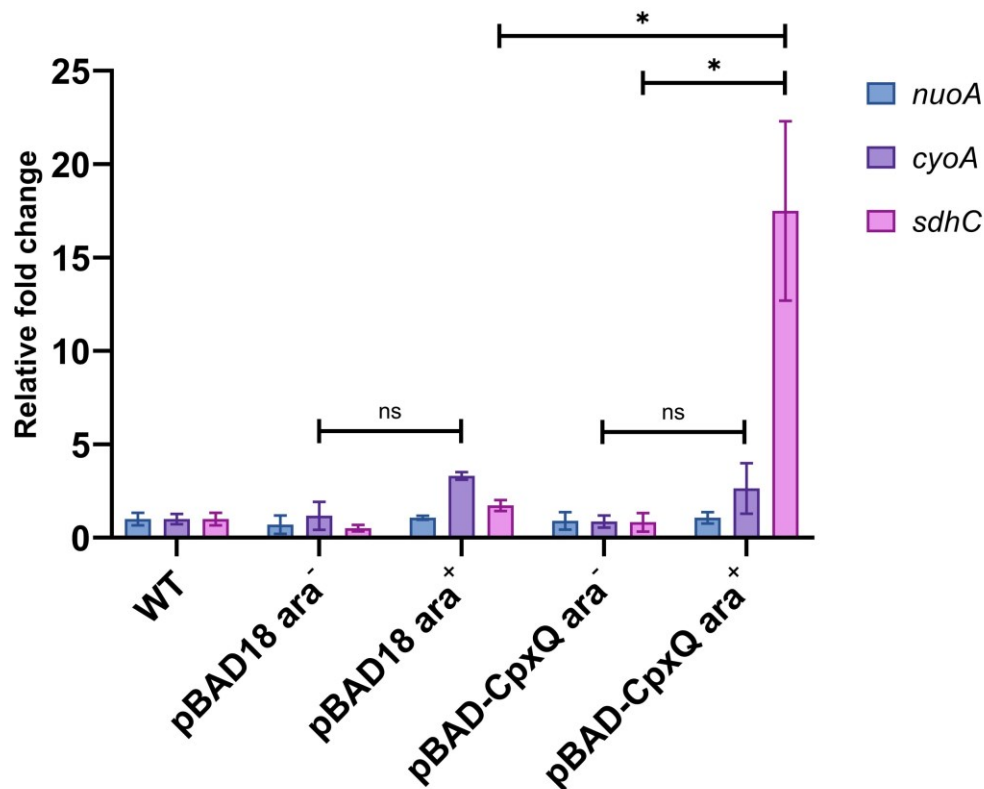
Figure 9. Overexpression of CpxQ sRNA affects the stability of *sdhC* mRNA. Strains of *E.coli* MC4100 carrying either arabinose-inducible empty pBAD18 vector, or the same vector expressing CpxQ sRNAwere subcultured into fresh LB medium after overnight growth in LB medium and grown with shaking at 37°C to a final OD_{600} of 0.35 to 0.4. 0.2% L-arabinose was used for CpxQ induction from the pBAD-CpxQ vector and all strains were grown for an additional 10min. RNA isolation, cDNA library generation and qPCR were performed as described in the Materials and Methods section. Data correspond to the mean values from three biological replicates in technical triplicates each. Error bars depict standard deviations (SDs). Statistical analyses were performed using Student's unpaired t-test, a P value of less than 0.05 was considered significant and represented by a *. Ns, not significant.

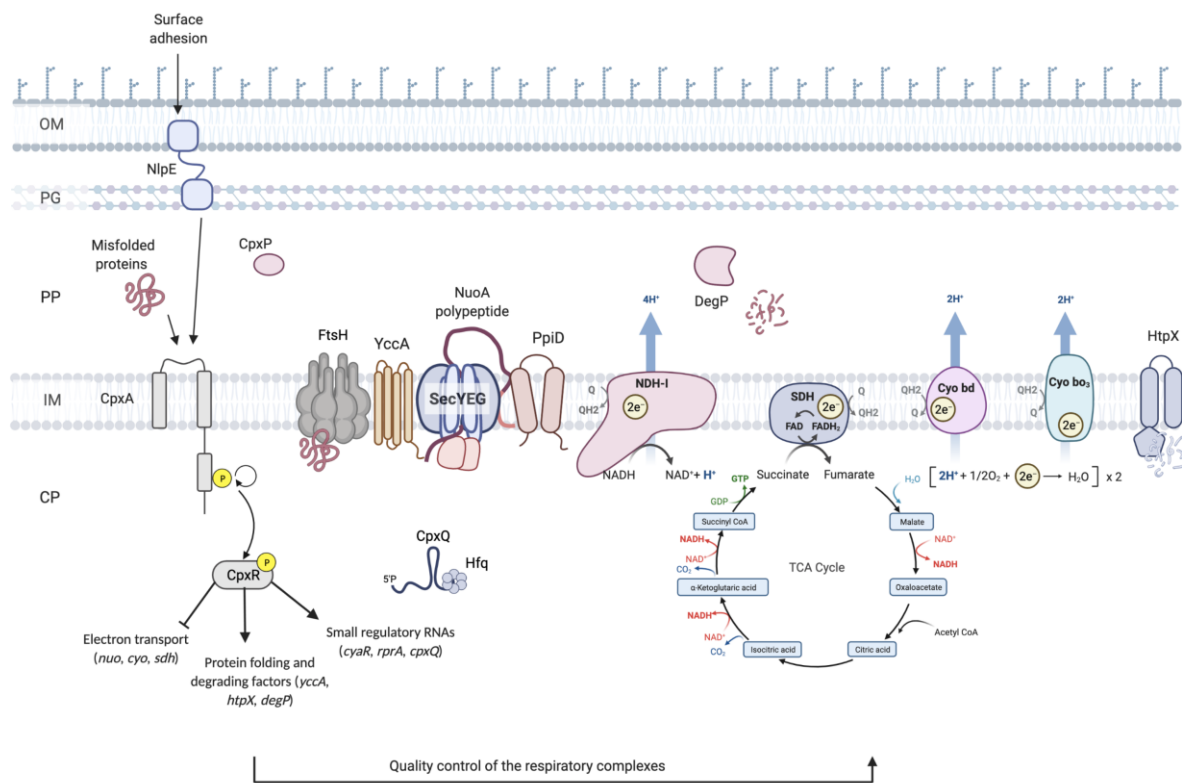**Figure 10. Model of the quality control of the ETC performed by the Cpx envelope stress response at the inner membrane of *E. coli*.** Upon activation of the Cpx response, CpxR represses the transcription of the operons encoding the NDH-I (*nuo*), cytochrome *bo₃* (*cyo*) and succinate dehydrogenase (*sdh*) respiratory complexes. In addition, the Cpx response regulates the biogenesis of these complexes beyond transcription through increased expression of protein folding and degrading factors, as well as upregulation of the sRNA synthesis. Cpx-regulated protein folding factors assist with the secretion and further insertion of integral parts of the ETC complexes, whereas the proteolytic factors maintain the adequate turnover and degradation of the misfolded or mislocalized proteins. The increased production of the CpxQ sRNA causes stabilization of the *sdhC* transcript through the unknown mechanism. OM, outer membrane; PG, peptidoglycan; PP, periplasm; CP, cytoplasm; 5'P, 5' monophosphate; Q, quinone; QH₂, quinol; H⁺, proton; NAD, nicotinamide adenine dinucleotide; FAD, flavin adenine dinucleotide; H₂O, water; O₂, molecular oxygen.

BIBLIOGRAPHY

1. Fakruddin M, Mohammad Mazumdar R, Bin Mannan KS, Chowdhury A, Hossain MN. 2013. Critical Factors Affecting the Success of Cloning, Expression, and Mass Production of Enzymes by Recombinant E. coli. ISRN Biotechnol 2013:590587.

2. Tenaillon O, Skurnik D, Picard B, Denamur E. 2010. The population genetics of commensal Escherichia coli. Nat Rev Microbiol 8:207–217.

3. Conway T, Cohen PS. 2015. Commensal and Pathogenic Escherichia coli Metabolism in the Gut. Microbiol Spectr 3.

4. Delmas J, Guillaume Dalmasso and Richard Bonnet, Bonnet GD and R. 2015. Escherichia coli: The Good, the Bad and the Ugly. Clin Microbiol Open Access 4.

5. Nataro JP, Kaper JB. 1998. Diarrheagenic Escherichia coli. Clin Microbiol Rev 11:142–201.

6. Silhavy TJ, Kahne D, Walker S. 2010. The bacterial cell envelope. Cold Spring Harb Perspect Biol 2:a000414.

7. Glauert AM, Thornley MJ. 1969. The topography of the bacterial cell wall. Annu Rev Microbiol 23:159–198.

8. Ruiz N, Kahne D, Silhavy TJ. 2006. Advances in understanding bacterial outer-membrane biogenesis. Nat Rev Microbiol 4:57–66.

9. Erridge C, Bennett-Guerrero E, Poxton IR. 2002. Structure and function of lipopolysaccharides. Microbes Infect 4:837–851.

10. Raetz CRH, Whitfield C. 2002. Lipopolysaccharide endotoxins. Annu Rev Biochem 71:635–700.

11. Whitfield C. 1988. Bacterial extracellular polysaccharides. Can J Microbiol 34:415–420.

12. Braun V. 1975. Covalent lipoprotein from the outer membrane of Escherichia coli.

Biochim Biophys Acta 415:335–377.

13.   Nikaido H. 1992. Porins and specific channels of bacterial outer membranes. Mol Microbiol 6:435–442.

14.   Luirink J, Yu Z, Wagner S, de Gier J-W. 2012. Biogenesis of inner membrane proteins in Escherichia coli. Biochim Biophys Acta 1817:965–976.

15.   Weiner JH, Li L. 2008. Proteome of the Escherichia coli envelope and technological challenges in membrane proteome analysis. Biochim Biophys Acta - Biomembr 1778:1698–1713.

16.   Albers R. 1999. Membrane Proteins, p. . *In* Siegel, G, Agranoff, B, Albers, R, Et al. (eds.), Basic Neurochemistry: Molecular, Cellular and Medical Aspects, 6th ed. Lippincott-Raven, Philadelphia.

17.   Allen KN, Entova S, Ray LC, Imperiali B. 2019. Monotopic Membrane Proteins Join the Fold. Trends Biochem Sci2018/10/15. 44:7–20.

18.   Liu D. 2014. Escherichia coli, p. 171–182. *In* Schmidt, T (ed.), Reference Module in Biomedical Sciences, 4th ed. Elsevier, Oxford.

19.   Miller SI, Salama NR. 2018. The gram-negative bacterial periplasm: Size matters. PLoS Biol 16:e2004935–e2004935.

20.   Duguay AR, Silhavy TJ. 2004. Quality control in the bacterial periplasm. Biochim Biophys Acta 1694:121–134.

21.   Typas A, Banzhaf M, Gross CA, Vollmer W. 2012. From the regulation of peptidoglycan synthesis to bacterial growth and morphology. Nat Rev Microbiol 10:123–136.

22.   Vollmer W, Blanot D, De Pedro MA. 2008. Peptidoglycan structure and architecture. FEMS Microbiol Rev 32:149–167.

23.   Reusch RN. 2012. Insights into the structure and assembly of Escherichia coli outer

membrane protein A. FEBS J 279:894–909.

24.   De Mot R, Vanderleyden J. 1994. The C-terminal sequence conservation between OmpA-related outer membrane proteins and MotB suggests a common function in both gram-positive and gram-negative bacteria, possibly in the interaction of these domains with peptidoglycan. Mol Microbiol. England.

25.   Koebnik R. 1995. Proposal for a peptidoglycan-associating alpha-helical motif in the C-terminal regions of some bacterial cell-surface proteins. Mol Microbiol. England.

26.   Asmar AT, Ferreira JL, Cohen EJ, Cho S-H, Beeby M, Hughes KT, Collet J-F. 2017. Communication across the bacterial cell envelope depends on the size of the periplasm. PLOS Biol 15:e2004303.

27.   Wall E, Majdalani N, Gottesman S. 2018. The Complex Rcs Regulatory Cascade. Annu Rev Microbiol 72:111–139.

28.   Bernal-Cabas M, Ayala JA, Raivio TL. 2015. The Cpx envelope stress response modifies peptidoglycan cross-linking via the L,D-transpeptidase LdtD and the novel protein YgaU. J Bacteriol 197:603–614.

29.   Stephenson K. 2005. Sec-dependent protein translocation across biological membranes: evolutionary conservation of an essential protein transport pathway (review). Mol Membr Biol 22:17–28.

30.   Lee PA, Tullman-Ercek D, Georgiou G. 2006. The bacterial twin-arginine translocation pathway. Annu Rev Microbiol 60:373–395.

31.   Berks BC. 1996. A common export pathway for proteins binding complex redox cofactors? Mol Microbiol 22:393–404.

32.   Natale P, Brüser T, Driessen AJMM. 2008. Sec- and Tat-mediated protein secretion across the bacterial cytoplasmic membrane-Distinct translocases and mechanisms. Biochim Biophys Acta 1778:1735–1756.

33. Ito K. 1992. SecY and integral membrane components of the Escherichia coli protein translocation system. Mol Microbiol 6:2423–2428.

34. Veenendaal AKJJ, van der Does C, Driessen AJMM. 2004. The protein-conducting channel SecYEG. Biochim Biophys Acta - Mol Cell Res 1694:81–95.

35. Pogliano JA, Beckwith J. 1994. SecD and SecF facilitate protein export in Escherichia coli. EMBO J 13:554–561.

36. Gardel C, Johnson K, Jacq A, Beckwith J. 1990. The secD locus of E.coli codes for two membrane proteins required for protein export. EMBO J 9:3209–3216.

37. Sagara K, Matsuyama S, Mizushima S. 1994. SecF stabilizes SecD and SecY, components of the protein translocation machinery of the Escherichia coli cytoplasmic membrane. J Bacteriol 176:4111–4116.

38. Matsuyama S, Fujita Y, Sagara K, Mizushima S. 1992. Overproduction, purification and characterization of SecD and SecF, integral membrane components of the protein translocation machinery of Escherichia coli. Biochim Biophys Acta 1122:77–84.

39. van Bloois E, Dekker HL, Fröderberg L, Houben ENGG, Urbanus ML, de Koster CG, de Gier J-WW, Luirink J. 2008. Detection of cross-links between FtsH, YidC, HflK/C suggests a linked role for these proteins in quality control upon insertion of bacterial inner membrane proteins. FEBS Lett 582:1419–1424.

40. Dalbey RE, Kuhn A. 2014. How YidC inserts and folds proteins across a membrane. Nat Struct Mol Biol 21:435–436.

41. Scotti PA, Urbanus ML, Brunner J, de Gier J-WL, von Heijne G, van der Does C, Driessen AJM, Oudega B, Luirink J. 2000. YidC, the Escherichia coli homologue of mitochondrial Oxa1p, is a component of the Sec translocase. EMBO J 19:542–549.

42. Price CE, Driessen AJM. 2010. Conserved negative charges in the transmembrane segments of subunit K of the NADH:ubiquinone oxidoreductase determine its

dependence on YidC for membrane insertion. J Biol Chem 285:3575–3581.

43.   Van der Laan M, Urbanus ML, Ten Hagen-Jongman CM, Nouwen N, Oudega B, Harms N, Driessen AJM, Luirink J. 2003. A conserved function of YidC in the biogenesis of respiratory chain complexes. Proc Natl Acad Sci U S A 100:5801–5806.

44.   van der Laan M, Bechtluft P, Kol S, Nouwen N, Driessen AJM. 2004. F1F0 ATP synthase subunit c is a substrate of the novel YidC pathway for membrane protein biogenesis . J Cell Biol 165:213–222.

45.   Du Plessis DJFF, Nouwen N, Driessen AJMM. 2006. Subunit a of cytochrome o oxidase requires both YidC and SecYEG for membrane insertion. J Biol Chem 281:12248–12252.

46.   Van Bloois E, Haan GJ, De Gier JW, Oudega B, Luirink J. 2006. Distinct requirements for translocation of the N-tail and C-tail of the Escherichia coli inner membrane protein CyoA. J Biol Chem 281:10002–10009.

47.   Yi L, Celebi N, Chen M, Dalbey RE. 2004. Sec/SRP requirements and energetics of membrane insertion of subunits a, b, and c of the Escherichia coli F1F0 ATP synthase. J Biol Chem 279:39260–39267.

48.   Kervinen M, Pätsi J, Finel M, Hassinen IE. 2004. A Pair of Membrane-Embedded Acidic Residues in the NuoK Subunit of Escherichia coli NDH-1, a Counterpart of the ND4L Subunit of the Mitochondrial Complex I, Are Required for High Ubiquinone Reductase Activity. Biochemistry 43:773–781.

49.   Kao M-C, Di Bernardo S, Nakamaru-Ogiso E, Miyoshi H, Matsuno-Yagi A, Yagi T. 2005. Characterization of the membrane domain subunit NuoJ (ND6) of the NADH-quinone oxidoreductase from Escherichia coli by chromosomal DNA manipulation. Biochemistry 44:3562–3571.

50.   Xie K, Dalbey RE. 2008. Inserting proteins into the bacterial cytoplasmic membrane

using the Sec and YidC translocases. Nat Rev Microbiol 6:234–244.

51.	Wullt B, Bergsten G, Connell H, Röllano P, Gebretsadik N, Hull R, Svanborg C. 2000. P fimbriae enhance the early establishment of Escherichia coli in the human urinary tract. Mol Microbiol 38:456–464.

52.	Tobe T, Sasakawa C. 2001. Role of bundle-forming pilus of enteropathogenic Escherichia coli in host cell adherence and in microcolony development. Cell Microbiol 3:579–585.

53.	Bina XR, Daniele P, Nathalie N, E. BJ. 2008. Vibrio cholerae RND Family Efflux Systems Are Required for Antimicrobial Resistance, Optimal Virulence Factor Production, and Colonization of the Infant Mouse Small Intestine. Infect Immun 76:3595–3605.

54.	Carlsson KE, Junfa L, J. EP, S. FM. 2007. Extracytoplasmic-Stress-Responsive Pathways Modulate Type III Secretion in Yersinia pseudotuberculosis. Infect Immun 75:3913–3924.

55.	Terashima H, Kojima S, Homma M. 2008. Flagellar motility in bacteria structure and function of flagellar motor. Int Rev Cell Mol Biol 270:39–85.

56.	Holmgren A, Kuehn MJ, Brändén CI, Hultgren SJ. 1992. Conserved immunoglobulin-like features in a family of periplasmic pilus chaperones in bacteria. EMBO J 11:1617–1622.

57.	Hung DL, Knight SD, Woods RM, Pinkner JS, Hultgren SJ. 1996. Molecular basis of two subfamilies of immunoglobulin-like chaperones. EMBO J 15:3792–3805.

58.	Hung DL, Raivio TL, Jones CH, Silhavy TJ, Hultgren SJ. 2001. Cpx signaling pathway monitors biogenesis and affects assembly and expression of P pili. EMBO J 20:1508–1518.

59.	Gruenheid S, Finlay BB. 2003. Microbial pathogenesis and cytoskeletal function.

Nature 422:775–781.

60.   Park H, Teja K, O'Shea JJ, Siegel RM. 2007. The Yersinia Effector Protein YpkA

Induces Apoptosis Independently of Actin Depolymerization. J Immunol 178:6426 LP

– 6434.

61.   Hemrajani C, Berger CN, Robinson KS, Marchès O, Mousnier A, Frankel G. 2010.

NleH effectors interact with Bax inhibitor-1 to block apoptosis during

enteropathogenic Escherichia coli infection. Proc Natl Acad Sci U S A2010/01/26.

107:3129–3134.

62.   Blasche S, Mörtl M, Steuber H, Siszler G, Nisa S, Schwarz F, Lavrik I, Gronewold

TMA, Maskos K, Donnenberg MS, Ullmann D, Uetz P, Kögl M. 2013. The E. coli

effector protein NleF is a caspase inhibitor. PLoS One2013/03/14. 8:e58937–e58937.

63.   Green ER, Mecsas J. 2016. Bacterial Secretion Systems: An Overview. Microbiol

Spectr 4:10.1128/microbiolspec.VMBF-0012–2015.

64.   Büttner D. 2012. Protein export according to schedule: architecture, assembly, and

regulation of type III secretion systems from plant- and animal-pathogenic bacteria.

Microbiol Mol Biol Rev 76:262–310.

65.   Logsdon LK, Mecsas J. 2003. Requirement of the Yersinia pseudotuberculosis

effectors YopH and YopE in colonization and persistence in intestinal and lymph

tissues. Infect Immun 71:4595–4607.

66.   Trülzsch K, Sporleder T, Igwe EI, Rüssmann H, Heesemann J. 2004. Contribution of

the major secreted yops of Yersinia enterocolitica O:8 to pathogenicity in the mouse

infection model. Infect Immun 72:5227–5234.

67.   Cascales E, Christie PJ. 2003. The versatile bacterial type IV secretion systems. Nat

Rev Microbiol 1:137–149.

68.   Hamilton HL, Dillard JP. 2006. Natural transformation of Neisseria gonorrhoeae: from

DNA donation to homologous recombination. Mol Microbiol 59:376–385.

69. Backert S, Meyer TF. 2006. Type IV secretion systems and their effectors in bacterial pathogenesis. Curr Opin Microbiol 9:207–217.

70. Russell AB, Peterson SB, Mougous JD. 2014. Type VI secretion system effectors: poisons with a purpose. Nat Rev Microbiol2014/01/02. 12:137–148.

71. Messens J, Collet JF, Van Belle K, Brosens E, Loris R, Wyns L. 2007. The oxidase DsbA folds a protein with a nonconsecutive disulfide. J Biol Chem 282:31302–31307.

72. Gilbert HF. 1990. Molecular and cellular aspects of thiol-disulfide exchange. Adv Enzymol Relat Areas Mol Biol 63:69–172.

73. Holmgren A, Fagerstedt M. 1982. The in vivo distribution of oxidized and reduced thioredoxin in Escherichia coli. J Biol Chem 257:6926–6930.

74. Arts IS, Gennaris A, Collet J-F. 2015. Reducing systems protecting the bacterial cell envelope from oxidative damage. FEBS Lett 589:1559–1568.

75. Bardwell JC, McGovern K, Beckwith J. 1991. Identification of a protein required for disulfide bond formation in vivo. Cell 67:581–589.

76. Wunderlich M, Glockshuber R. 1993. Redox properties of protein disulfide isomerase (DsbA) from Escherichia coli. Protein Sci 2:717–726.

77. Zapun A, Creighton TE, Bardwell JCA, Creighton TE. 1993. The Reactive and Destabilizing Disulfide Bond of DsbA, a Protein Required for Protein Disulfide Bond Formation in Vivo. Biochemistry 32:5083–5092.

78. Berkmen M. 2012. Production of disulfide-bonded proteins in Escherichia coli. Protein Expr Purif 82:240–251.

79. Joly JC, Swartz JR. 1997. In vitro and in vivo redox states of the Escherichia coli periplasmic oxidoreductases DsbA and DsbC. Biochemistry 36:10067–10072.

80. Denoncin K, Collet JF. 2013. Disulfide bond formation in the bacterial periplasm:

Major achievements and challenges ahead. Antioxidants Redox Signal 19:63–71.

81.   Bader M, Muse W, Ballou DP, Gassner C, Bardwell JCA. 1999. Oxidative protein folding is driven by the electron transport system. Cell 98:217–227.

82.   Bader MW, Xie T, Yu CA, Bardwell JCA. 2000. Disulfide bonds are generated by quinone reduction. J Biol Chem 275:26082–26088.

83.   Rietsch A, Bessette P, Georgiou G, Beckwith J. 1997. Reduction of the periplasmic disulfide bond isomerase, DsbC, occurs by passage of electrons from cytoplasmic thioredoxin. J Bacteriol 179:6602–6608.

84.   Justice SS, Hunstad DA, Harper JR, Duguay AR, Pinkner JS, Bann J, Frieden C, Silhavy TJ, Hultgren SJ. 2005. Periplasmic peptidyl prolyl cis-trans isomerases are not essential for viability, but SurA is required for pilus biogenesis in Escherichia coli. J Bacteriol 187:7680–7686.

85.   Göthel SF, Marahiel MA. 1999. Peptidyl-prolyl cis-trans isomerases, a superfamily of ubiquitous folding catalysts. Cell Mol Life Sci 55:423–436.

86.   Dartigalongue C, Raina S. 1998. A new heat-shock gene, ppiD, encodes a peptidyl-prolyl isomerase required for folding of outer membrane proteins in Escherichia coli. EMBO J 17:3968–3980.

87.   Matern Y, Barion B, Behrens-Kneip S. 2010. PpiD is a player in the network of periplasmic chaperones in Escherichia coli. BMC Microbiol 10:251.

88.   Fürst M, Zhou Y, Merfort J, Müller M. 2018. Involvement of PpiD in Sec-dependent protein translocation. Biochim Biophys acta Mol cell Res 1865:273–280.

89.   Antonoaea R, Fürst M, Nishiyama K-II, Müller M. 2008. The periplasmic chaperone PpiD interacts with secretory proteins exiting from the SecYEG translocon. Biochemistry 47:5649–5656.

90.   Clark DP, Pazdernik NJ. 2016. Chapter 9 - Proteomics, p. 295–333. *In* Clark, DP,

Pazdernik, NJBT-B (Second E (eds.), . Academic Cell, Boston.

91. Olivares AO, Baker TA, Sauer RT. 2016. Mechanistic insights into bacterial AAA+ proteases and protein-remodelling machines. Nat Rev Microbiol2015/12/07. 14:33–44.

92. Sauer RT, Bolon DN, Burton BM, Burton RE, Flynn JM, Grant RA, Hersch GL, Joshi SA, Kenniston JA, Levchenko I, Neher SB, Oakes ESC, Siddiqui SM, Wah DA, Baker TA. 2004. Sculpting the proteome with AAA(+) proteases and disassembly machines. Cell 119:9–18.

93. Ito K, Akiyama Y. 2005. Cellular functions, mechanism of action, and regulation of FtsH protease. Annu Rev Microbiol 59:211–231.

94. Ogura T, Inoue K, Tatsuta T, Suzaki T, Karata K, Young K, Su L-H, Fierke CA, Jackman JE, Raetz CRH, Coleman J, Tomoyasu T, Matsuzawa H. 1999. Balanced biosynthesis of major membrane components through regulated degradation of the committed enzyme of lipid A biosynthesis by the AAA protease FtsH (HflB) in Escherichia coli. Mol Microbiol 31:833–844.

95. Führer F, Langklotz S, Narberhaus F. 2006. The C-terminal end of LpxC is required for degradation by the FtsH protease. Mol Microbiol 59:1025–1036.

96. Krzywda S, Brzozowski AM, Verma C, Karata K, Ogura T, Wilkinson AJ. 2002. The crystal structure of the AAA domain of the ATP-dependent protease FtsH of Escherichia coli at 1.5 A resolution. Structure 10:1073–1083.

97. Saikawa N, Akiyama Y, Ito K. 2004. FtsH exists as an exceptionally large complex containing HflKC in the plasma membrane of Escherichia coli. J Struct Biol 146:123–129.

98. Bieniossek C, Schalch T, Bumann M, Meister M, Meier R, Baumann U. 2006. The molecular architecture of the metalloprotease FtsH. Proc Natl Acad Sci U S A 103:3066–3071.

99. Langklotz S, Baumann U, Narberhaus F. 2012. Structure and function of the bacterial AAA protease FtsH. Biochim Biophys Acta - Mol Cell Res 1823:40–48.

100. Gottesman S. 1996. Proteases and their targets in Escherichia coli. Annu Rev Genet 30:465–506.

101. Kihara A, Akiyama Y, Ito K. 1998. Different pathways for protein degradation by the FtsH/HflKC membrane-embedded protease complex: An implication from the interference by a mutant form of a new substrate protein, YccA. J Mol Biol 279:175–188.

102. Akiyama Y, Ito K. 1998. FtsH protease, p. 1502 –1504. *In* Barret, AJ, Rawlings, ND, Woessner, JF (eds.), Handbook of Proteolytic Enzymes. London: Academic Press.

103. Herman C, Prakash S, Lu CZ, Matouschek A, Gross CA. 2003. Lack of a robust unfoldase activity confers a unique level of substrate specificity to the universal AAA protease FtsH. Mol Cell 11:659–669.

104. Akiyama Y, Kihara A, Ito K. 1996. Subunit a of proton ATPase F0 sector is a substrate of the FtsH protease in Escherichia coli. FEBS Lett 399:26–28.

105. Kihara A, Akiyama Y, Ito K. 1995. FtsH is required for proteolytic elimination of uncomplexed forms of SecY, an essential protein translocase subunit. Proc Natl Acad Sci U S A 92:4532–4536.

106. Akiyama Y, Ogura T, Ito K. 1994. Involvement of FtsH in protein assembly into and through the membrane. I. Mutations that reduce retention efficiency of a cytoplasmic reporter. J Biol Chem 269:5218–5224.

107. Chiba S, Akiyama Y, Ito K. 2002. Membrane protein degradation by FtsH can be initiated from either end. J Bacteriol 184:4775–4782.

108. Sakoh M, Ito K, Akiyama Y. 2005. Proteolytic activity of HtpX, a membrane-bound and stress-controlled protease from Escherichia coli. J Biol Chem 280:33305–33310.

109. Chiba S, Ito K, Akiyama Y. 2006. The Escherichia coli plasma membrane contains two PHB (prohibitin homology) domain protein complexes of opposite orientations. Mol Microbiol 60:448–457.

110. Shimohata N, Chiba S, Saikawa N, Ito K, Akiyama Y. 2002. The Cpx stress response system of Escherichia coli senses plasma membrane proteins and controls HtpX, a membrane protease with a cytosolic active site. Genes to Cells 7:653–662.

111. Akiyama Y. 2009. Quality Control of Cytoplasmic Membrane Proteins in Escherichia coli. J Biochem 146:449–454.

112. Yoshitani K, Hizukuri Y, Akiyama Y. 2019. An in vivo protease activity assay for investigating the functions of the Escherichia coli membrane protease HtpX. FEBS Lett 593:842–851.

113. Kihara A, Akiyama Y, Ito K. 1996. A protease complex in the Escherichia coli plasma membrane: HflKC (HflA) forms a complex with FtsH (HflB), regulating its proteolytic activity against SecY. EMBO J 15:6122–6131.

114. Akiyama Y, Kihara A, Mori H, Ogura T, Ito K. 1998. Roles of the periplasmic domain of Escherichia coli FtsH (HflB) in protein interactions and activity modulation. J Biol Chem 273:22326–22333.

115. Kihara A, Ito K. 1998. Translocation, Folding, and Stability of the HflKC Complex with Signal Anchor Topogenic Sequences. J Biol Chem 273:29770–29775.

116. Clausen T, Southan C, Ehrmann M. 2002. The HtrA family of proteases: Implications for protein composition and cell fate. Mol Cell 10:443–455.

117. Ge X, Wang R, Ma J, Liu Y, Ezemaduka AN, Chen PR, Fu X, Chang Z. 2014. DegP primarily functions as a protease for the biogenesis of β-barrel outer membrane proteins in the Gram-negative bacterium Escherichia coli. FEBS J 281:1226–1240.

118. Spiess C, Beil A, Ehrmann M. 1999. A temperature-dependent switch from chaperone

to protease in a widely conserved heat shock protein. Cell 97:339–347.

119. Vogt SL, Raivio TL. 2012. Just scratching the surface: an expanding view of the Cpx envelope stress response. FEMS Microbiol Lett 326:2–11.

120. Rouvière PE, De Las Peñas A, Mecsas J, Lu CZ, Rudd KE, Gross CA. 1995. rpoE, the gene encoding the second heat-shock sigma factor, sigma E, in Escherichia coli. EMBO J 14:1032–1042.

121. Hews CL, Cho T, Rowley G, Raivio TL. 2019. Maintaining Integrity Under Stress: Envelope Stress Response Regulation of Pathogenesis in Gram-Negative Bacteria. Front Cell Infect Microbiol 9:1–25.

122. Danese PN, Silhavy TJ. 1997. The sigma(E) and the Cpx signal transduction systems control the synthesis of periplasmic protein-folding enzymes in Escherichia coli. Genes Dev 11:1183–1193.

123. Raivio TL, Silhavy TJ. 1997. Transduction of envelope stress in Escherichia coli by the Cpx two-component system. J Bacteriol 179:7724–7733.

124. Raivio TL, Silhavy TJ. 2001. Periplasmic stress and ECF sigma factors. Annu Rev Microbiol 55:591–624.

125. Delhaye A, Collet J-F, Laloux G. 2019. A Fly on the Wall: How Stress Response Systems Can Sense and Respond to Damage to Peptidoglycan. Front Cell Infect Microbiol 9.

126. Grabowicz M, Silhavy TJ. 2017. Envelope Stress Responses: An Interconnected Safety Net. Trends Biochem Sci 42:232–242.

127. Pogliano J, Lynch AS, Belin D, Lin ECC, Beckwith J, Genetics M, Universitaire CM, Francisco SS. 1997. Regulation of Escherichia coli cell envelope proteins involved in protein folding and degradation by the Cpx two-component system. Genes Dev 11:1169–1182.

128. Raivio TL. 2014. Everything old is new again: An update on current research on the Cpx envelope stress response. Biochim Biophys Acta - Mol Cell Res 1843:1529–1541.

129. Danese PN, Silhavy TJ. 1998. CpxP, a stress-combative member of the Cpx regulon. J Bacteriol 180:831–839.

130. Raivio TL, Popkin DL, Silhavy TJ. 1999. The Cpx Envelope Stress Response Is Controlled by Amplification and Feedback Inhibition. J Bacteriol 181:5263 LP – 5272.

131. Danese PN, Snyder WB, Cosma CL, Davis LJB, Silhavy TJ. 1995. The Cpx two-component signal transduction pathway of Escherichia coli regulates transcription of the gene specifying the stress-inducible periplasmic protease, DegP. Genes Dev 9:387–398.

132. Otto K, Silhavy TJ. 2002. Surface sensing and adhesion of Escherichia coli controlled by the Cpx-signaling pathway. Proc Natl Acad Sci U S A 99:2287–2292.

133. Hirano Y, Hossain MM, Takeda K, Tokuda H, Miki K. 2007. Structural Studies of the Cpx Pathway Activator NlpE on the Outer Membrane of Escherichia coli. Structure 15:963–976.

134. Shimizu T, Ichimura K, Noda M. 2015. The Surface Sensor NlpE of Enterohemorrhagic Escherichia coli Contributes to Regulation of the Type III Secretion System and Flagella by the Cpx Response to Adhesion. Infect Immun 84:537–549.

135. Delhaye A, Laloux G, Collet J-FF. 2019. The lipoprotein NlpE is a cpx sensor that serves as a sentinel for protein sorting and folding defects in the escherichia coli envelope. J Bacteriol 209:1–12.

136. Grabowicz M, Silhavy TJ. 2017. Redefining the essential trafficking pathway for outer membrane lipoproteins. Proc Natl Acad Sci 114:4769 LP – 4774.

137. Nakayama S, Watanabe H. 1995. Involvement of cpxA, a sensor of a two-component

regulatory system, in the pH-dependent regulation of expression of Shigella sonnei virF gene. J Bacteriol 177:5062–5069.

138. Mileykovskaya E, Dowhan W. 1997. The Cpx two-component signal transduction pathway is activated in Escherichia coli mutant strains lacking phosphatidylethanolamine. J Bacteriol 179:1029–1034.

139. Jones CH, Danese PN, Pinkner JS, Silhavy TJ, Hultgren SJ. 1997. The chaperone-assisted membrane release and folding pathway is sensed by two signal transduction systems. EMBO J 16:6394–6406.

140. Kohanski MA, Dwyer DJ, Wierzbowski J, Cottarel G, Collins JJ. 2008. Mistranslation of membrane proteins and two-component system activation trigger antibiotic-mediated cell death. Cell 135:679–690.

141. Peng W, Andreas K, E. DR. 2010. Global Change of Gene Expression and Cell Physiology in YidC-Depleted Escherichia coli. J Bacteriol 192:2193–2209.

142. Danese PN, Silhavy TJ. 1997. The σ(E) and the Cpx signal transduction systems control the synthesis of periplasmic protein-folding enzymes in Escherichia coli. Genes Dev 11:1183–1193.

143. Raivio TL, Laird MW, Joly JC, Silhavy TJ. 2000. Tethering of CpxP to the inner membrane prevents spheroplast induction of the Cpx envelope stress response. Mol Microbiol 37:1186–1197.

144. Cosma CL, Danese PN, Carlson JH, Silhavy TJ, Snyder WB. 1995. Mutational activation of the Cpx signal transduction pathway of Escherichia coli suppresses the toxicity conferred by certain envelope-associated stresses. Mol Microbiol 18:491–505.

145. Raivio TL, Leblanc SKD, Price NL. 2013. The Escherichia coli Cpx envelope stress response regulates genes of diverse function that impact antibiotic resistance and membrane integrity. J Bacteriol 195:2755–2767.

146. Beisel CL, Storz G. 2010. Base pairing small RNAs and their roles in global regulatory networks. FEMS Microbiol Rev 34:866–882.

147. Vogt SL, Evans AD, Guest RL, Raivio TL. 2014. The Cpx envelope stress response regulates and is regulated by small noncoding RNAs. J Bacteriol 196:4229–4238.

148. Wassarman KM. 2002. Small RNAs in bacteria: Diverse regulators of gene expression in response to environmental changes. Cell 109:141–144.

149. Vogel J, Luisi BF. 2011. Hfq and its constellation of RNA. Nat Rev Microbiol 9:578–589.

150. Storz G, Vogel J, Wassarman KM. 2011. Regulation by Small RNAs in Bacteria: Expanding Frontiers. Mol Cell 43:880–891.

151. Fröhlich KS, Gottesman S. 2018. Small Regulatory RNAs in the Enterobacterial Response to Envelope Damage and Oxidative Stress. Regul with RNA Bact Archaea 211–228.

152. Roberts JW. 2019. Mechanisms of Bacterial Transcription Termination. J Mol Biol 431:4030–4039.

153. Denham EL. 2020. The Sponge RNAs of bacteria – How to find them and their role in regulating the post-transcriptional network. Biochim Biophys Acta - Gene Regul Mech 1863:194565.

154. Jens H, Gianluca M, Jörg V, Susan G, Gisela S, T. LS, Deborah H, HÖR J, MATERA G, VOGEL J, GOTTESMAN S, STORZ G. 2020. Trans-Acting Small RNAs and Their Effects on Gene Expression in Escherichia coli and Salmonella enterica. EcoSal Plus 9.

155. Nara F-B, Lionello B, Gisela S, Kai P. 2018. Sponges and Predators in the Small RNA World. Microbiol Spectr 6:6.4.11.

156. Grüll MP, Massé E. 2019. Mimicry, deception and competition: The life of competing

endogenous RNAs. WIREs RNA 10:e1525.

157.   Soper T, Mandin P, Majdalani N, Gottesman S, Woodson SA. 2010. Positive

regulation by small RNAs and the role of Hfq. Proc Natl Acad Sci U S A 107:9602–

9607.

158.   Geissmann TA, Touati D. 2004. Hfq, a new chaperoning role: binding to messenger

RNA determines access for small RNA regulator. EMBO J 23:396–405.

159.   Valentin-Hansen P, Eriksen M, Udesen C. 2004. The bacterial Sm-like protein Hfq: a

key player in RNA transactions. Mol Microbiol 51:1525–1533.

160.   Smirnov A, Förstner KU, Holmqvist E, Otto A, Günster R, Becher D, Reinhardt R,

Vogel J. 2016. Grad-seq guides the discovery of ProQ as a major small RNA-binding

protein. Proc Natl Acad Sci U S A 113:11591–11596.

161.   Melamed S, Adams PP, Zhang A, Zhang H, Storz G. 2020. RNA-RNA Interactomes

of ProQ and Hfq Reveal Overlapping and Competing Roles. Mol Cell 77:411-425.e7.

162.   Smirnov A, Wang C, Drewry LL, Vogel J. 2017. Molecular mechanism of mRNA

repression in trans by a ProQ-dependent small RNA. EMBO J 36:1029–1045.

163.   Morita T, Maki K, Aiba H. 2005. RNase E-based ribonucleoprotein complexes:

mechanical basis of mRNA destabilization mediated by bacterial noncoding RNAs.

Genes Dev 19:2176–2186.

164.   Waters LS, Storz G. 2009. Regulatory RNAs in bacteria. Cell 136:615–628.

165.   Massé E, Gottesman S. 2002. A small RNA regulates the expression of genes involved

in iron metabolism in Escherichia coli. Proc Natl Acad Sci U S A 99:4620–4625.

166.   Beisel CL, Storz G. 2011. The base pairing RNA Spot 42 participates in a multi-output

feedforward loop to help enact catabolite repression in Escherichia coli. Mol Cell

41:286–297.

167.   Møller T, Franch T, Udesen C, Gerdes K, Valentin-Hansen P. 2002. Spot 42 RNA

mediates discoordinate expression of the E. coli galactose operon. Genes Dev 16:1696–1706.

168. Balbontín R, Fiorini F, Figueroa-Bossi N, Casadesús J, Bossi L. 2010. Recognition of heptameric seed sequence underlies multi-target regulation by RybB small RNA in Salmonella enterica. Mol Microbiol 78:380–394.

169. Bossi L, Figueroa-Bossi N. 2007. A small RNA downregulates LamB maltoporin in Salmonella. Mol Microbiol 65:799–810.

170. Bouvier M, Sharma CM, Mika F, Nierhaus KH, Vogel J. 2008. Small RNA binding to 5' mRNA coding region inhibits translational initiation. Mol Cell 32:827–837.

171. Johansen J, Rasmussen AA, Overgaard M, Valentin-Hansen P. 2006. Conserved small non-coding RNAs that belong to the sigmaE regulon: role in down-regulation of outer membrane proteins. J Mol Biol 364:1–8.

172. Papenfort K, Bouvier M, Mika F, Sharma CM, Vogel J. 2010. Evidence for an autonomous 5′ target recognition domain in an Hfq-associated small RNA. Proc Natl Acad Sci 107:20435 LP – 20440.

173. Papenfort K, Pfeiffer V, Mika F, Lucchini S, Hinton JCD, Vogel J. 2006. σE-dependent small RNAs of Salmonella respond to membrane stress by accelerating global omp mRNA decay. Mol Microbiol 62:1674–1688.

174. Udekwu KI, Darfeuille F, Vogel J, Reimegård J, Holmqvist E, Wagner EGH. 2005. Hfq-dependent regulation of OmpA synthesis is mediated by an antisense RNA. Genes Dev 19:2355–2366.

175. Udekwu KI, Wagner EGH. 2007. Sigma E controls biogenesis of the antisense RNA MicA. Nucleic Acids Res2007/01/31. 35:1279–1288.

176. Chao Y, Vogel J. 2016. A 3' UTR-Derived Small RNA Provides the Regulatory Noncoding Arm of the Inner Membrane Stress Response. Mol Cell 61:352–363.

177. Grabowicz M, Koren D, Silhavy TJ. 2016. The Cpxq sRNA negatively regulates skp to prevent mistargeting of β-barrel outer membrane proteins into the cytoplasmic membrane. MBio 7:1–8.

178. Bianco CM, Fröhlich KS, Vanderpool CK. 2018. Bacterial cyclopropane fatty acid synthase mRNA is targeted by activating and repressing small RNAs. J Bacteriol 201:1–20.

179. Guest RL, Wang J, Wong JL, Raivio TL. 2017. A Bacterial Stress Response Regulates Respiratory Protein Complexes To Control Envelope Stress Adaptation 199:1–14.

180. Iosub IA, van Nues RW, McKellar SW, Nieken KJ, Marchioretto M, Sy B, Tree JJ, Viero G, Granneman S. 2020. Hfq CLASH uncovers sRNA-target interaction networks linked to nutrient availability adaptation. Elife 9:1–33.

181. Adams PP, Baniulyte G, Esnault C, Chegireddy K, Singh N, Monge M, Dale RK, Storz G, Wade JT. 2021. Regulatory roles of Escherichia coli 5' UTR and ORF-internal RNAs detected by 3' end mapping. Elife 10:e62438.

182. Anraku Y. 1988. Bacterial electron transport chains. Annu Rev Biochem 57:101–132.

183. Yoshida M, Muneyuki E, Hisabori T. 2001. ATP synthase - a marvellous rotary engine of the cell. Nat Rev Mol Cell Biol 2:669–677.

184. Price CE, Driessen AJMM. 2010. Biogenesis of membrane bound respiratory complexes in Escherichia coli. Biochim Biophys Acta - Mol Cell Res 1803:748–766.

185. Borisov VBB, Murali R, Verkhovskaya MLL, Bloch DAA, Han H, Gennis RBB, Verkhovsky MII. 2011. Aerobic respiratory chain of Escherichia coli is not allowed to work in fully uncoupled mode. Proc Natl Acad Sci 108:17320–17324.

186. Kaila VRII, Wikström M. 2021. Architecture of bacterial respiratory chains. Nat Rev Microbiol 19:319–330.

187. Kaila VRIRI, Verkhovsky MII, Wikström M. 2010. Proton-Coupled Electron Transfer

in Cytochrome Oxidase. Chem Rev 110:7062–7081.

188. Leif H, Sled VD, Ohnishi T, Weiss H, Friedrich T. 1995. Isolation and characterization of the proton-translocating NADH: ubiquinone oxidoreductase from Escherichia coli. Eur J Biochem 230:538–548.

189. Kerscher S, Dröse S, Zickermann V, Brandt U. 2008. The three families of respiratory NADH dehydrogenases. Results Probl Cell Differ 45:185–222.

190. Brandt U. 2006. Energy converting NADH:quinone oxidoreductase (complex I). Annu Rev Biochem 75:69–92.

191. Braun M, Bungert S, Friedrich T. 1998. Characterization of the overproduced NADH dehydrogenase fragment of the NADH:ubiquinone oxidoreductase (complex I) from Escherichia coli. Biochemistry 37:1861–1867.

192. Friedrich T, Dekovic DK, Burschel S. 2016. Assembly of the Escherichia coli NADH:ubiquinone oxidoreductase (respiratory complex I). Biochim Biophys Acta - Bioenerg 1857:214–223.

193. Baranova EA, Holt PJ, Sazanov LA. 2007. Projection Structure of the Membrane Domain of Escherichia coli Respiratory Complex I at 8 Å Resolution. J Mol Biol 366:140–154.

194. Hofhaus G, Weiss H, Leonard K. 1991. Electron microscopic analysis of the peripheral and membrane parts of mitochondrial NADH dehydrogenase (Complex I). J Mol Biol 221:1027–1043.

195. Guénebaut V, Schlitt A, Weiss H, Leonard K, Friedrich T. 1998. Consistent structure between bacterial and mitochondrial NADH:ubiquinone oxidoreductase (complex I). J Mol Biol 276:105–112.

196. Py B, Barras F. 2010. Building Fe-S proteins: Bacterial strategies. Nat Rev Microbiol 8:436–446.

197. Lestienne P, Desnuelle C. 1999. Complex II or Succinate: Quinone Oxidoreductase and Pathology BT - Mitochondrial Diseases: Models and Methods, p. 87–95. *In* Lestienne, P (ed.), . Springer Berlin Heidelberg, Berlin, Heidelberg.

198. Yankovskaya V, Horsefield R, Törnroth S, Luna-Chavez C, Miyoshi H, Léger C, Byrne B, Cecchini G, Iwata S. 2003. Architecture of succinate dehydrogenase and reactive oxygen species generation. Science (80-) 299:700–704.

199. Tran QM, Rothery RA, Maklashina E, Cecchini G, Weiner JH. 2006. The quinone binding site in Escherichia coli succinate dehydrogenase is required for electron transfer to the heme b. J Biol Chem 281:32310–32317.

200. Nakamura K, Yamaki M, Sarada M, Nakayama S, Vibat CR, Gennis RB, Nakayashiki T, Inokuchi H, Kojima S, Kita K. 1996. Two hydrophobic subunits are essential for the heme b ligation and functional assembly of complex II (succinate-ubiquinone oxidoreductase) from Escherichia coli. J Biol Chem 271:521–527.

201. Yankovskaya V, Horsefield R, Törnroth S, Luna-chavez C, Miyoshi H, Léger C, Byrne B, Cecchini G, Iwata S. 2003. Architecture of Succinate Dehydrogenase and Reactive Oxygen Species Generation Published by : American Association for the Advancement of Science Stable URL : http://www.jstor.org/stable/3833442. Science (80-) 299:700–704.

202. Baba T, Ara T, Hasegawa M, Takai Y, Okumura Y, Baba M, Datsenko KA, Tomita M, Wanner BL, Mori H. 2006. Construction of Escherichia coli K-12 in-frame, single-gene knockout mutants: The Keio collection. Mol Syst Biol 2.

203. Silhavy T., Berman M., Enquist L. 1984. Experiments with gene fusions. Cold Spring Harbor Laboratory.

204. Kitagawa M, Ara T, Arifuzzaman M, Ioka-Nakamichi T, Inamoto E, Toyonaga H, Mori H. 2005. Complete set of ORF clones of Escherichia coli ASKA library (a

complete set of E. coli K-12 ORF archive): unique resources for biological research. DNA Res an Int J rapid Publ reports genes genomes 12:291–299.

205. Wong JL, Vogt SL, Raivio TL. 2013. Using reporter genes and the Escherichia coli ASKA overexpression library in screens for regulators of the gram negative envelope stress response. Methods Mol Biol 966:337–357.

206. Price NL, Raivio TL. 2009. Characterization of the Cpx regulon in Escherichia coli strain MC4100. J Bacteriol 191:1798–1815.

207. Macritchie DM, Ward JD, Nevesinjac AZ, Raivio TL. 2008. Activation of the Cpx envelope stress response down-regulates expression of several locus of enterocyte effacement-encoded genes in enteropathogenic Escherichia coli. Infect Immun2008/01/28. 76:1465–1475.

208. Weinberg ED. 1959. Gradient Agar Plates. Am Biol Teach 21:347–350.

209. Münch R, Hiller K, Grote A, Scheer M, Klein J, Schobert M, Jahn D. 2005. Virtual Footprint and PRODORIC: an integrative framework for regulon prediction in prokaryotes. Bioinformatics 21:4187–4189.

210. Ammar EM, Wang X, Rao C V. 2018. Regulation of metabolism in Escherichia coli during growth on mixtures of the non-glucose sugars: arabinose, lactose, and xylose. Sci Rep 8:609.

211. Chang D-E, Smalley DJJ, Tucker DLL, Leatham MPP, Norris WEE, Stevenson SJJ, Anderson ABB, Grissom JEE, Laux DCC, Cohen PSS, Conway T. 2004. Carbon nutrition of Escherichia coli in the mouse intestine. Proc Natl Acad Sci U S A 101:7427 LP – 7432.

212. McNeil MBB, Clulow JSS, Wilf NMM, Salmond GPCPC, Fineran PCC. 2012. SdhE is a conserved protein required for flavinylation of succinate dehydrogenase in bacteria. J Biol Chem2012/04/03. 287:18418–18428.

213. Prüss BMM, Nelms JMM, Park C, Wolfe AJJ. 1994. Mutations in NADH:ubiquinone oxidoreductase of Escherichia coli affect growth on mixed amino acids. J Bacteriol 176:2143–2150.

214. Guest RLRL. 2017. Regulation of respiration by the Cpx response in enteropathogenic Escherichia coli. University of Alberta.

215. Yamamoto K, Ishihama A. 2006. Characterization of copper-inducible promoters regulated by CpxA/CpxR in Escherichia coli. Biosci Biotechnol Biochem 70:1688–1695.

216. Jones CH, Dexter P, Evans AK, Liu C, Hultgren SJ, Hruby DE. 2002. Escherichia coli DegP Protease Cleaves between Paired Hydrophobic Residues in a Natural Substrate: the PapA Pilin. J Bacteriol 184:5762 LP – 5771.

217. Massé E, Vanderpool CK, Gottesman S. 2005. Effect of RyhB small RNA on global iron use in Escherichia coli. J Bacteriol 187:6962–6971.

218. Mann M, Wright PR, Backofen R. 2017. IntaRNA 2.0: enhanced and customizable prediction of RNA-RNA interactions. Nucleic Acids Res 45:W435–W439.

219. Wright PR, Georg J, Mann M, Sorescu DA, Richter AS, Lott S, Kleinkauf R, Hess WR, Backofen R. 2014. CopraRNA and IntaRNA: predicting small RNA targets, networks and interaction domains. Nucleic Acids Res 42:W119-23.

220. Busch A, Richter AS, Backofen R. 2008. IntaRNA: efficient prediction of bacterial sRNA targets incorporating target site accessibility and seed regions. Bioinformatics 24:2849–2856.

221. Raden M, Ali SM, Alkhnbashi OS, Busch A, Costa F, Davis JA, Eggenhofer F, Gelhausen R, Georg J, Heyne S, Hiller M, Kundu K, Kleinkauf R, Lott SC, Mohamed MM, Mattheis A, Miladi M, Richter AS, Will S, Wolff J, Wright PR, Backofen R. 2018. Freiburg RNA tools: a central online resource for RNA-focused research and

teaching. Nucleic Acids Res 46:W25–W29.

222. Fröhlich KS, Papenfort K. 2020. Regulation outside the box: New mechanisms for small RNAs. Mol Microbiol2020/08/13. 114:363–366.

223. Fröhlich KS, Papenfort K, Fekete A, Vogel J. 2013. A small RNA activates CFA synthase by isoform-specific mRNA stabilization. EMBO J 32:2963–2979.

224. Gruber AR, Bernhart SH, Lorenz R. 2015. The ViennaRNA web services. Methods Mol Biol 1269:307–326.

225. ENGLESBERG E, ANDERSON RL, WEINBERG R, LEE N, HOFFEE P, HUTTENHAUER G, BOYER H. 1962. L-Arabinose-sensitive, L-ribulose 5-phosphate 4-epimerase-deficient mutants of Escherichia coli. J Bacteriol 84:137–146.

226. Cecchini G, Schroder I, Gunsalus RP, Maklashina E. 2002. Succinate dehydrogenase and fumarate reductase from Escherichia coli. Biochim Biophys ACTA-BIOENERGETICS 1553:140–157.

227. Hederstedt L, Rutberg L. 1981. Succinate-dehydrogenase - a comparative review. Microbiol Rev 45:542–555.

228. De Wulf P, McGuire AM, Liu X, Lin ECC. 2002. Genome-wide profiling of promoter recognition by the two-component response regulator CpxR-P in Escherichia coli. J Biol Chem 277:26652–26661.

229. Shen J, Gunsalus RP. 1997. Role of multiple ArcA recognition sites in anaerobic regulation of succinate dehydrogenase (sdhCDAB) gene expression in Escherichia coli. Mol Microbiol 26:223–236.

230. Park S -J, Tseng C -P, Gunsalus RP. 1995. Regulation of succinate dehydrogenase sdhCDAB operon expression in Escherichia coli in response to carbon supply and anaerobiosis: role of ArcA and Fnr. Mol Microbiol 15:473–482.

231. Surmann K, Stopp M, Wörner S, Dhople VM, Völker U, Unden G, Hammer E. 2020.

Fumarate dependent protein composition under aerobic and anaerobic growth conditions in Escherichia coli. J Proteomics 212:103583.

232. Zheng D, Constantinidou C, Hobman JL, Minchin SD. 2004. Identification of the CRP regulon using in vitro and in vivo transcriptional profiling. Nucleic Acids Res 32:5874–5893.

233. Zhang Z, Gosset G, Barabote R, Gonzalez CS, Cuevas WA, Saier MHJ. 2005. Functional interactions between the carbon and iron utilization regulators, Crp and Fur, in Escherichia coli. J Bacteriol 187:980–990.

234. Kumar R, Shimizu K. 2011. Transcriptional regulation of main metabolic pathways of cyoA, cydB, fnr, and fur gene knockout Escherichia coli in C-limited and N-limited aerobic continuous cultures. Microb Cell Fact 10:3.

235. Desnoyers G, Massé E. 2012. Noncanonical repression of translation initiation through small RNA recruitment of the RNA chaperone Hfq. Genes Dev 26:726–739.

236. Isaac DD, Pinkner JS, Hultgren SJ, Silhavy TJ. 2005. The extracytoplasmic adaptor protein CpxP is degraded with substrate by DegP. Proc Natl Acad Sci U S A 102:17775–17779.

237. Engl C, Beek A Ter, Bekker M, de Mattos JT, Jovanovic G, Buck M. 2011. Dissipation of proton motive force is not sufficient to induce the phage shock protein response in Escherichia coli. Curr Microbiol 62:1374–1385.

238. Bongaerts J, Zoske S, Weidner U, Linden G. 1995. Transcriptional regulation of the proton translocating NADH dehydrogenase (nuoA-N) of Escherichia coli by electron acceptors, electron donors and gene regulators. Mol Microbiol 16:521–534.

239. Aussel L, Pierrel F, Loiseau L, Lombard M, Fontecave M, Barras F. 2014. Biosynthesis and physiology of coenzyme Q in bacteria. Biochim Biophys Acta - Bioenerg 1837:1004–1011.

240. Au DC, Gennis RB. 1987. Cloning of the cyo locus encoding the cytochrome o terminal oxidase complex of Escherichia coli. J Bacteriol 169:3237 LP – 3242.

241. Mitchell AM, Silhavy TJ. 2019. Envelope stress responses: balancing damage repair and toxicity. Nat Rev Microbiol 17:417–428.

242. Raivio TL. 2018. Regulation of proteolysis in the Gram-negative bacterial envelope. J Bacteriol 200:1–6.

243. Karp G. 2008. Cell and Molecular Biology: Concepts and Experiments, 5th ed. John Wiley & Sons, Limited.

244. Minárik P, Tomásková N, Kollárová M, Antalík M. 2002. Malate dehydrogenases-- structure and function. Gen Physiol Biophys 21:257–265.

245. Matsushita K, Ohnishi T, Kaback HR. 1987. NADH-ubiquinone oxidoreductases of the Escherichia coli aerobic respiratory chain. Biochemistry 26:7732–7737.

246. Kao M-CC, Nakamaru-Ogiso E, Matsuno-Yagi A, Yagi T. 2005. Characterization of the membrane domain subunit NuoK (ND4L) of the NADH-quinone oxidoreductase from Escherichia coli. Biochemistry 44:9545–9554.

247. Van Stelten J, Silva F, Belin D, Silhavy TJ. 2009. Effects of antibiotics and a proto-oncogene homolog on destruction of protein translocator SecY. Science (80-) 325:753–756.

248. Bittner LM, Westphal K, Narberhaus F. 2015. Conditional proteolysis of the membrane protein YfgM by the FtsH protease depends on a novel N-terminal degron. J Biol Chem 290:19367–19378.

249. Leiser OP, Charlson ES, Gerken H, Misra R. 2012. Reversal of the ΔdegP Phenotypes by a Novel rpoE Allele of Escherichia coli. PLoS One 7:e33979.

250. McDowall KJ, Lin-Chao S, Cohen SN. 1994. A+U content rather than a particular nucleotide order determines the specificity of RNase E cleavage. J Biol Chem

269:10790–10796.

251. Mackie GA. 2013. RNase E: at the interface of bacterial RNA processing and decay. Nat Rev Microbiol 11:45–57.

252. Krulwich TA. 1986. Bioenergetics of alkalophilic bacteria. J Membr Biol 89:113–125.

253. Padan E, Zilberstein D, Rottenberg H. 1976. The proton electrochemical gradient in Escherichia coli cells. Eur J Biochem 63:533–541.

254. Booth IR. 1985. Regulation of cytoplasmic pH in bacteria. Microbiol Rev 49:359–378.

255. Ohyama T, Igarashi K, Kobayashi H. 1994. Physiological role of the chaA gene in sodium and calcium circulations at a high pH in Escherichia coli. J Bacteriol 176:4311–4315.

256. Casadaban MJ. 1976. Transposition and fusion of the lac genes to selected promoters in Escherichia coli using bacteriophage lambda and Mu. J Mol Biol 104:541–555.

257. Levine MM, Bergquist EJ, Nalin DR, Waterman DH, Hornick RB, Young CR, Sotman S. 1978. Escherichia coli strains that cause diarrhoea but do not produce heat-labile or heat-stable enterotoxins and are non-invasive. Lancet (London, England) 1:1119–1122.

258. Datsenko KA, Wanner BL. 2000. One-step inactivation of chromosomal genes in Escherichia coli K-12 using PCR products. Proc Natl Acad Sci U S A 97:6640–6645.

259. 1985. Eperiments with Gene Fusions. J Basic Microbiol 25:350.

260. Mayer MP. 1995. A new set of useful cloning and expression vectors derived from pBlueScript. Gene 163:41–46.